Exact resummations in the theory of hydrodynamic turbulence. III. Scenarios for anomalous scaling and intermittency

Victor L'vov [1,3,*] and Itamar Procaccia [2,†]
[1]*Department of Physics of Complex Systems, The Weizmann Institute of Science, Rehovot 76100, Israel*
[2]*Department of Chemical Physics, The Weizmann Institute of Science, Rehovot 76100, Israel*
[3]*Institute of Automation and Electrometry, Academy of Science of Russia, 630090, Novosibirsk, Russia*
(Received 6 July 1995)

Elements of the analytic structure of anomalous scaling and intermittency in fully developed hydrodynamic turbulence are described. We focus here on the structure functions of velocity differences that satisfy inertial range scaling laws $S_n(R)\sim R^{\zeta_n}$, and the correlation of energy dissipation $K_{\epsilon\epsilon}(R)\sim R^{-\mu}$. The goal is to understand from first principles what is the mechanism that is responsible for changing the exponents ζ_n and μ from their classical Kolmogorov values. In paper II of this series [V. S. L'vov and I. Procaccia, Phys. Rev. E **52**, 3858 (1995)] it was shown that the existence of an ultraviolet scale (the dissipation scale η) is associated with a spectrum of anomalous exponents that characterize the ultraviolet divergences of correlations of gradient fields. The leading scaling exponent in this family was denoted Δ. The exact resummation of ladder diagrams resulted in a "bridging relation," which determined Δ in terms of ζ_2: $\Delta=2-\zeta_2$. In this paper we continue our analysis and show that nonperturbative effects may introduce multiscaling (i.e., ζ_n not linear in n) with the renormalization scale being the infrared outer scale of turbulence L. It is shown that deviations from the classical Kolmogorov 1941 theory scaling of $S_n(R)$ ($\zeta_n\neq n/3$) must appear if the correlation of dissipation is mixing (i.e., $\mu>0$). We suggest possible scenarios for multiscaling, and discuss the implication of these scenarios on the values of the scaling exponents ζ_n and their "bridge" with μ.

PACS number(s): 47.27.−i

I. INTRODUCTION

This paper is the fourth in a series of papers [1–3]. The aim of this series is to lay out the analytic basis for the description of scaling properties in fully developed hydrodynamic turbulence. We are concerned here with the statistical properties of turbulence in terms of averages over the fields of the fluid. The fundamental field in hydrodynamics is the fluid's Eulerian velocity, denoted as $\mathbf{u}(\mathbf{r},t)$ where $\mathbf{r}$ is a point in d-dimensional space (usually $d=2$ or 3) and t is the time. The statistical quantities that have attracted decades of experimental and theoretical attention (see, for example, [4–8]) are the structure functions of velocity differences, denoted as $S_n(R)$:

$$S_n(R)=\langle|\,\mathbf{u}(\mathbf{r}+\mathbf{R},t)-\mathbf{u}(\mathbf{r},t)|^n\rangle, \tag{1.1}$$

where $\langle\rangle$ stands for a suitably defined ensemble average. It has been asserted for a long time that the structure functions depend on R as power laws:

$$S_n(R)\propto R^{\zeta_n}, \tag{1.2}$$

when R is inside the so-called "inertial range," i.e., $\eta\ll R\ll L$. Here η and L are respectively the inner (viscous) and outer (energy containing) scale of turbulence. One of the major questions in fundamental turbulence research is whether the scaling exponents ζ_n are correctly predicted by the classical Kolmogorov 1941 theory [4] (known as K41) in which $\zeta_n=n/3$, or whether these exponents deviate from $n/3$ as has been indicated by experiments. In particular we want to know how the exponents ζ_n may manifest the phenomenon of "multiscaling" with ζ_n being a nonlinear function of n.

Experimental research has not confined itself to the measurement of the structure functions of velocity differences. Gradient fields have featured as well. For example, the correlation function of the energy dissipation field has been studied extensively. The dissipation field $\epsilon(\mathbf{r},t)$ is defined as

$$\epsilon(\mathbf{r},t)\equiv\frac{\nu}{2}[\nabla_\alpha u_\beta(\mathbf{r},t)+\nabla_\beta u_\alpha(\mathbf{r},t)]^2, \tag{1.3}$$

with ν being the kinematic viscosity. The correlation function of the dissipation field $K_{\epsilon\epsilon}(R)$ is

$$K_{\epsilon\epsilon}(R)=\langle\hat{\epsilon}(\mathbf{r}+\mathbf{R},t)\hat{\epsilon}(\mathbf{r},t)\rangle, \tag{1.4}$$

where $\hat{\epsilon}(\mathbf{r},t)=\epsilon(\mathbf{r},t)-\bar{\epsilon}$. Here and below $\bar{\epsilon}\equiv\langle\epsilon\rangle$. Experiments appeared to show [5–8] that $K_{\epsilon\epsilon}(R)$ decays according to a power law,

$$K_{\epsilon\epsilon}(R)\sim R^{-\mu},\quad \eta\ll R\ll L, \tag{1.5}$$

with μ having a numerical value of 0.2−0.3. The analytic derivation of this law from the equations of fluid mechanics and the calculation of the numerical value of the scaling exponent μ have been among the elusive goals of theoretical research.

In paper 0 of this series [1] we reviewed the literature [9–11] with the aim of introducing the student to the available techniques. That paper did not present any new results.

*Electronic address: fnlvov@wis.weizmann.ac.il
†Electronic address: cfprocac@weizmann.weizmann.ac.il

In paper I of this series [2] we dealt with the perturbative theory of the correlation, response, and structure functions of hydrodynamic turbulence. The main result of that paper (and see also [12]) was that after appropriate resummations and renormalizations the perturbative theory for these quantities is finite order by order. All the integrals appearing in the theory are convergent both in the ultraviolet and in the infrared limits. This means that there is no perturbative mechanism to introduce a length scale into the theory of the structure functions. In turn this result indicated that as far as the perturbative theory is concerned there is no mechanism to shift the exponents ζ_n away from their K41 values. Of course, nonperturbative effects may furnish such a mechanism and therefore in paper II [3] we turned to the analysis of nonperturbative effects. It was shown there that the renormalized perturbation theory for correlation functions that include velocity derivatives (to second or higher power) exhibit in their perturbation expansion a logarithmic dependence on the viscous scale η [13,14]. In this way the inner scale of turbulence appears explicitly in the analytic theory. The perturbative series could be resummed to obtain integrodifferential equations for some many-point objects of the theory. These equations have also nonperturbative scale-invariant solutions that may be represented as power laws of η to some exponents Δ. We argued [15] that if $\Delta<\Delta_c$ where

$$\Delta_c=2-\zeta_2 \tag{1.6}$$

(a situation referred to as the "subcritical scenario"), then K41 scaling is asymptotically exact for infinite Re. In this case $K_{\epsilon\epsilon}(R)\sim\bar{\epsilon}^2(\eta/R)^{2(4/3-\Delta)}$, and the exponent μ is identified with $2(4/3-\Delta)$. The renormalization length is then the inner length η.

In paper II it was shown that the exponent Δ takes on exactly the critical value $\Delta=\Delta_c$ given by (1.6), and the subcritical scenario is not realized. The consequences of this are manifold. In particular this criticality of the theory means that K41 is not realized for high Reynolds numbers. This understanding is one of the main goals of the present paper.

We wish to elucidate the possible mechanisms for anomalous (non-K41) scaling of the structure functions in the theory of turbulence in fluids whose dynamics is described by the Navier-Stokes equations. The main point is that although order by order our renormalized perturbation series for S_n can be shown to converge and be independent of the inner or outer scales, the criticality of Δ leads to an outer scale dependence of the whole series. In other words, the series diverges when $L\to\infty$. Precisely how the series diverges with L determines the numerical values of the various scaling exponents. The full analysis of this nonperturbative mechanism is not easy. In particular we learn that the inertial range scaling depends sensitively on the crossover to dissipative behavior of various objects. These crossovers are governed by the various dissipative scales that appear in the theory. The calculation of these scales from first principles calls for the development of the theory in the viscous regime, and this has not been done yet to our knowledge. Therefore we have to make assumptions about the dissipative scales. Different assumptions lead to different scenarios for multiscaling with different nonlinear dependence of ζ_n on n.

Having a nonperturbative problem at hand, we need to base the analysis on a global constraint. We show that a useful analysis of anomalous scaling can be developed on the basis of the so-called "balance equations," which are nonperturbative. In Sec. II we derive the balance equations [(2.24), (2.25)] by writing the equations of motion for the structure function $S_n(R)$ and of related quantities. These equations, in the stationary state, exhibit a balance between a convective (interaction) term, which is denoted as $D_n(R)$, and a dissipative term, denoted by $J_n(R)$, which is the cross correlation between the energy dissipation $\hat{\epsilon}$ and $(n-2)$ velocity differences across a scale R. Both terms are expressed as many-point correlation functions that depend on many coordinates, but some of these coordinates are the same. This last fact leads to the main strategy of this paper, which is to understand the fusion rules that describe the scaling of many-point correlation functions when some of their coordinates fuse together. When this happens the distance between the coordinates crosses the dissipative scale, and at that very moment the ultraviolet divergences are picked up. This is the point where the dissipative behavior of various objects comes into play. The information learned in paper II gives us an important part of the fusion rules, but they have to be completed with information about the viscous scales. The simplest scenario follows from an assumption that there exists a unique dissipative scale η that governs the crossover to dissipative behavior of all the objects. In such a scenario we can compute the dissipative term $J_n(R)$ and the correlation function $K_{\epsilon\epsilon}(R)$ in terms of exponents ζ_n that can multiscale with $\zeta_n\propto\sqrt{n}$ for large n. We believe that this assumption is too strong. The other scenario follows from allowing a multiplicity of dissipative scales. Basing our arguments on the Kolmogorov refined similarity hypothesis we develop an alternative (but also multiscaling) scenario with different predictions for the large n dependence of $\zeta_n\propto n$. It is not impossible that a first principles theory of the viscous scaling behavior (a theory that still awaits developing) will lead to yet a third scenario. The main message here is that we identify the fundamental mechanism for the appearance of the outer scale in the theory, and this, in principle, allows multiscaling.

The fusion rules are developed in Secs. III–V. In Sec. III we show that the exponent Δ of paper II is indeed the relevant exponent for describing pair coalescence. In Sec. IV we discuss four-point correlations and their two-point fusion rules. This leads to the calculation of the correlation $K_{\epsilon\epsilon}(R)$ and the dissipative term J_4. In Sec. V we discuss the fusion rules of n-point correlation functions, leading to the evaluation of $J_n(R)$. A consequence of this calculation is the derivation of the dynamical scaling exponents z_n describing the characteristic decay time $\tau_n(R)\propto R^{z_n}$ of n-point, n-time correlation functions of Belinicher-L'vov (BL) velocity differences.

In Sec. VI we turn to the evaluation of the interaction term $D_n(R)$ and the resulting implications on ζ_n. The terms in the diagrammatic series for D_n converge order by order, demonstrating the perturbative locality of eddy interaction. Using the fusion rules we demonstrated locality also in the nonperturbative sense. This accomplishes the technical identification of the concept of "cascade" of energy flux down the scales. It also leads to the evaluation

$$D_n(R)=b_n\frac{dS_{n+1}(R)}{dR}, \tag{1.7}$$

with an unknown numerical coefficient b_n. Within the first scenario this evaluation of D_n leads to the scaling exponents of the β model. Within the second scenario it leads to multiscaling. Also the first scenario does not rule out multiscaling, if this evaluation of D_n is an overestimate. We propose that there may exist a delicate cancellation in this evaluation with $d_n=0$. The next order evaluation is

$$D_n(R)=d_n\frac{S_n(R)S_3(R)}{S_2(R)R}. \tag{1.8}$$

This evaluation leads unequivocally to multiscaling.

In order to compute the scaling exponents ζ_n we need to know D_n very precisely, coefficients and all. Not having an exact theory for D_n we resort in Sec. VII to modeling. This part of the paper is not rigorous, and the results of Sec. VII should be considered therefore as tentative. Section VIII has a summary and some discussion of the road ahead.

Throughout the text we may refer to equations appearing in papers 0, I, or II. When we do so we denote them as Eqs. (0-n), (I-n), (II-p), etc.

II. DERIVATION OF THE BALANCE EQUATIONS

Some of the most important nonperturbative constraints on the statistical theory of turbulence are the balance equations (also known as the moment equations) for the structure functions. These equations are derived in this section and used in later sections to deduce the scenarios for multiscaling in the structure functions. Before we derive the equations we introduce the statistical objects that appear naturally in the discussion.

A. Structure functions and related quantities

In this subsection we define quantities that are related to the structure functions $S_n(R)$. It is common in experiments to measure only the longitudinal structure functions [5]. For theoretical treatment these quantities are not necessarily the most convenient since they are not invariant to rotations. It is useful therefore to introduce some related objects that have simple transformation properties under rotations and inversions. The first one is the scalar quantity, which is appropriate for even orders of S_n. To keep in mind its scalar nature we will denote it as $\mathring{S}_{2m}(R)$ and define it in Eulerian terms as

$$\mathring{S}_{2m}(R)\equiv\langle|\delta\mathbf{u}(\mathbf{r}_0|\mathbf{R},t)|^{2m}\rangle,\quad \mathbf{R}\equiv\mathbf{r}-\mathbf{r}_0, \tag{2.1}$$

where

$$\delta\mathbf{u}(\mathbf{r}_0|\mathbf{R},t)\equiv\mathbf{u}(\mathbf{r}_0+\mathbf{R},t)-\mathbf{u}(\mathbf{r}_0,t) \tag{2.2}$$

is a simultaneous Eulerian velocity difference. The quantity $\mathring{S}_{2m}(R)$ is analytic. For odd order structure functions we introduce a vector object $\mathbf{S}_{2m+1}(\mathbf{R})$ according to

$$S^{\alpha}_{2m+1}(\mathbf{R})\equiv\langle\delta u_\alpha(\mathbf{r}_0|\mathbf{R},t)|\delta\mathbf{u}(\mathbf{r}_0|\mathbf{R},t)|^{2m}\rangle. \tag{2.3}$$

Here and below we will use Greek indices to indicate vector and tensor components, and Roman indices to indicate the order of the quantity. The placement of indices as subscripts or superscripts has no meaning, and is chosen for convenience.

For isotropic turbulence the vector $S^{\alpha}_{2m+1}(\mathbf{R})$ can only be oriented along $\mathbf{R}$. This allows us to introduce a scalar quantity $S_{2m+1}(R)$, which depends on the magnitude of R:

$$S^{\alpha}_{2m+1}(\mathbf{R})=\frac{R_\alpha}{R}S_{2m+1}(R). \tag{2.4}$$

Lastly we will need also the tensor objects $S^{\alpha\beta}_{2m+2}(\mathbf{R})$:

$$S^{\alpha\beta}_{2m+2}(\mathbf{R})\equiv\langle\delta u_\alpha(\mathbf{r}_0|\mathbf{R},t)\,\delta u_\beta(\mathbf{r}_0|\mathbf{R},t)|\delta\mathbf{u}(\mathbf{r}_0|\mathbf{R},t)|^{2m}\rangle. \tag{2.5}$$

Note that the objects introduced in (2.1), (2.3), and (2.5) involve an arbitrary number of velocity fields but only two spatial points separated by $\mathbf{R}$. We refer to them loosely as "two-point" correlation functions of velocity differences. The theory below calls for the introduction of three-point functions as well. It is best to define them using the four-point functions:

$$T^{\alpha\beta}_{2m+2}(\mathbf{R}_1,\mathbf{R}_2,\mathbf{R})\equiv\langle\delta u_\alpha(\mathbf{r}_0|\mathbf{R}_1,t)\,\delta u_\beta(\mathbf{r}_0|\mathbf{R}_2,t)|\delta\mathbf{u}(\mathbf{r}_0|\mathbf{R},t)|^{2m}\rangle, \tag{2.6}$$

$$T^{\alpha\beta\gamma}_{2m+3}(\mathbf{R}_1,\mathbf{R}_2,\mathbf{R})\equiv\langle\delta u_\alpha(\mathbf{r}_0|\mathbf{R}_1,t)\,\delta u_\beta(\mathbf{r}_0|\mathbf{R}_2,t)\,\delta u_\gamma(\mathbf{r}_0|\mathbf{R},t)|\times\delta\mathbf{u}(\mathbf{r}_0|\mathbf{R},t)|^{2m}\rangle, \tag{2.7}$$

$$T^{\alpha\beta\gamma\delta}_{2m+4}(\mathbf{R}_1,\mathbf{R}_2,\mathbf{R})\equiv\langle\delta u_\alpha(\mathbf{r}_0|\mathbf{R}_1,t)\,\delta u_\beta(\mathbf{r}_0|\mathbf{R}_2,t)\,\delta u_\gamma(\mathbf{r}_0|\mathbf{R},t)\times\delta u_\delta(\mathbf{r}_0|\mathbf{R},t)|\delta\mathbf{u}(\mathbf{r}_0|\mathbf{R},t)|^{2m}\rangle. \tag{2.8}$$

We will see that the theory produces expressions involving these quantities with two of the arguments being identical (i.e., $\mathbf{R}_1=\mathbf{R}_2$, etc.). This fact will lead to the study of fusion rules in later sections.

B. The balance equations

In this subsection we derive the balance equation that relates structure functions to correlation functions involving the dissipation field. We start by deriving some equations of motion for the quantities defined above.

Our starting point is the Navier-Stokes equations for an incompressible fluid:

$$\frac{\partial\mathbf{u}(\mathbf{r},t)}{\partial t}+[\mathbf{u}(\mathbf{r},t)\cdot\boldsymbol{\nabla}]\mathbf{u}(\mathbf{r},t)-\nu\nabla^2\mathbf{u}(\mathbf{r},t)-\boldsymbol{\nabla}p(\mathbf{r},t)=\mathbf{f}(\mathbf{r},t),$$

$$\boldsymbol{\nabla}\cdot\mathbf{u}=0. \tag{2.9}$$

For simplicity we will choose the forcing such that $\boldsymbol{\nabla}\cdot\mathbf{f}=0$. This equation can be rewritten in terms of the Belinicher-L'vov velocities $\mathbf{v}(\mathbf{r}_0,\mathbf{r},t)$ defined by Eq. (I-2.2) as follows:

$$\frac{\partial \mathbf{v}(\mathbf{r}_0|\mathbf{r},t)}{\partial t}+[\mathbf{w}(\mathbf{r}_0|\mathbf{r},t)\cdot\nabla]\mathbf{w}(\mathbf{r}_0|\mathbf{r},t)-\nu\nabla^2\mathbf{w}(\mathbf{r}_0|\mathbf{r},t)$$
$$-\nabla\tilde{p}(\mathbf{r}_0|\mathbf{r},t)=\tilde{\mathbf{f}}(\mathbf{r}_0|\mathbf{r},t), \tag{2.10}$$

where we also have the incompressibility condition $\nabla\cdot\mathbf{w}=0$. Here $\mathbf{w}$ is the BL velocity difference

$$\mathbf{w}(\mathbf{r}_0|\mathbf{r},t)\equiv\mathbf{v}(\mathbf{r}_0|\mathbf{r},t)-\mathbf{v}(\mathbf{r}_0|\mathbf{r}_0,t), \tag{2.11}$$

and $\tilde{p}(\mathbf{r}_0|\mathbf{r},t)$, $\tilde{\mathbf{f}}(\mathbf{r}_0|\mathbf{r},t)$ are BL-transformed pressure and forcing (for more detail, see Sec. III A of paper I). Applying the transverse projector $\overleftrightarrow{\mathbf{P}}$ this equation takes on the form

$$\frac{\partial \mathbf{v}(\mathbf{r}_0|\mathbf{r},t)}{\partial t}+\overleftrightarrow{\mathbf{P}}[\mathbf{w}(\mathbf{r}_0|\mathbf{r},t)\cdot\nabla]\mathbf{w}(\mathbf{r}_0|\mathbf{r},t)-\nu\nabla^2\mathbf{w}(\mathbf{r}_0|\mathbf{r},t)$$
$$=\tilde{\mathbf{f}}(\mathbf{r}_0|\mathbf{r},t). \tag{2.12}$$

The application of $\overleftrightarrow{\mathbf{P}}$ to any given vector field $\mathbf{a}(\mathbf{r})$ is nonlocal, and has the form

$$[\overleftrightarrow{\mathbf{P}}\mathbf{a}(\mathbf{r})]_\alpha=\int d\mathbf{r}'P_{\alpha\beta}(\mathbf{r}-\mathbf{r}')a_\beta(\mathbf{r}'), \tag{2.13}$$

where $P_{\alpha\beta}(\mathbf{r}-\mathbf{r}')$ is

$$P_{\alpha\beta}(\mathbf{r}-\mathbf{r}')=\delta_{\alpha\beta}\delta(\mathbf{r}-\mathbf{r}')-\frac{1}{4\pi}\left[\frac{\delta_{\alpha\beta}}{|\mathbf{r}-\mathbf{r}'|^3}-3\frac{(r_\alpha-r'_\alpha)(r_\beta-r'_\beta)}{|\mathbf{r}-\mathbf{r}'|^5}\right]. \tag{2.14}$$

Next we consider Eq. (2.12) at two spatial points, $\mathbf{r}$ and $\mathbf{r}_0$. Subtracting the two equations we get

$$\frac{\partial w_\alpha(\mathbf{r}_0|\mathbf{r},t)}{\partial t}+\int d\mathbf{r}'[P_{\alpha\beta}(\mathbf{r}-\mathbf{r}')-P_{\alpha\beta}(\mathbf{r}_0-\mathbf{r}')]w_\gamma$$
$$\times(\mathbf{r}_0|\mathbf{r}',t)(\nabla_{r'})_\gamma w_\beta(\mathbf{r}_0|\mathbf{r}',t)$$
$$=\nu[\nabla_r^2+\nabla_{r_0}^2]w_\alpha(\mathbf{r}_0|\mathbf{r},t)+\tilde{f}_\alpha(\mathbf{r}_0|\mathbf{r},t)-\tilde{f}_\alpha(\mathbf{r}_0|\mathbf{r}_0,t), \tag{2.15}$$

where $(\nabla_r)_\gamma\equiv\partial/\partial r_\gamma$. We introduce now the shorthand notation w^2 and w^{2m} in situations in which the arguments are $(\mathbf{r}_0|\mathbf{r},t)$:

$$|\mathbf{w}(\mathbf{r}_0|\mathbf{r},t)|^2\equiv w^2,\quad |\mathbf{w}(\mathbf{r}_0|\mathbf{r},t)|^{2m}\equiv w^{2m}. \tag{2.16}$$

When other arguments appear they will be displayed explicitly. In terms of these quantities the structure functions (2.1)–(2.3) are written as

$$\mathring{S}_{2m}(R)\equiv\langle w^{2m}\rangle, \tag{2.17}$$

$$\mathbf{S}_{2m+1}(R)\equiv\langle\mathbf{w}w^{2m}\rangle. \tag{2.18}$$

where again $\mathbf{R}=\mathbf{r}-\mathbf{r}_0$ and $\mathbf{w}$ without arguments means $\mathbf{w}(\mathbf{r}_0|\mathbf{r},t)$. Next observe that

$$\frac{\partial w^{2m}}{\partial t}=2mw^{2(m-1)}\mathbf{w}\cdot\frac{\partial\mathbf{w}}{\partial t}. \tag{2.19}$$

Evaluate now the scalar product obtained from Eq. (2.15) by multiplying it on the left by $2mw^{2(m-1)}\mathbf{w}$. Using Eq. (2.19) this is written exactly as

$$\frac{\partial\mathring{S}_{2m}(R)}{\partial t}+D_{2m}(R)=J_{2m}(R)+Q_{2m}(R), \tag{2.20}$$

where we denoted

$$D_{2m}(R)\equiv 2m\int d\mathbf{r}_1P_{\alpha\beta}(\mathbf{r}_1)\frac{\partial}{\partial r_{1\gamma}}\langle w^{2(m-1)}$$
$$\times w_\alpha[w_\gamma(\mathbf{r}_0|\mathbf{r}+\mathbf{r}_1,t)w_\beta(\mathbf{r}_0|\mathbf{r}+\mathbf{r}_1,t)$$
$$-w_\gamma(\mathbf{r}_0|\mathbf{r}_0+\mathbf{r}_1,t)w_\beta(\mathbf{r}_0|\mathbf{r}_0+\mathbf{r}_1,t)]\rangle, \tag{2.21}$$

$$J_{2m}(R)\equiv 2m\nu\langle w^{2(m-1)}w_\alpha[\nabla_r^2+\nabla_{r_0}^2]w_\alpha\rangle, \tag{2.22}$$

$$Q_{2m}(R)\equiv 2m\langle w^{2(m-1)}w_\alpha[f_\alpha(\mathbf{r}_0|\mathbf{r},t)-f_\alpha(\mathbf{r}_0|\mathbf{r}_0,t)]\rangle. \tag{2.23}$$

In deriving the equation for D_{2m} we used the incompressibility condition (which is not available in the Burgers equation) and performed changes of variables in the integrals according to $\mathbf{r}'-\mathbf{r}=\mathbf{r}_1$ and $\mathbf{r}'-\mathbf{r}_0=\mathbf{r}_1$. In the stationary state $\partial\mathring{S}_{2m}(R)/\partial t=0$, and we can write the scalar balance equation:

$$D_{2m}(R)=J_{2m}(R)+Q_{2m}(R). \tag{2.24}$$

Next we need to derive vectorial balance equations for $\mathbf{S}_{2m+1}$. Repeating similar steps we end up with

$$\mathbf{D}_{2m+1}(\mathbf{R})=\mathbf{J}_{2m+1}(\mathbf{R})+\mathbf{Q}_{2m+1}(\mathbf{R}), \tag{2.25}$$

where

$$D^\delta_{2m+1}(\mathbf{R})=2m\int d\mathbf{r}_1P_{\alpha\beta}(\mathbf{r}_1)\frac{\partial}{\partial r_{1\gamma}}\langle w^{2(m-1)}w_\delta w_\alpha[w_\gamma(\mathbf{r}_0|\mathbf{r}+\mathbf{r}_1,t)w_\beta(\mathbf{r}_0|\mathbf{r}+\mathbf{r}_1,t)-w_\gamma(\mathbf{r}_0|\mathbf{r}_0+\mathbf{r}_1,t)w_\beta(\mathbf{r}_0|\mathbf{r}_0+\mathbf{r}_1,t)]\rangle$$
$$+\int d\mathbf{r}_1P_{\delta\beta}(\mathbf{r}_1)\frac{\partial}{\partial r_{1\gamma}}\langle w^{2m}[w_\gamma(\mathbf{r}_0|\mathbf{r}+\mathbf{r}_1,t)w_\beta(\mathbf{r}_0|\mathbf{r}+\mathbf{r}_1,t)-w_\gamma(\mathbf{r}_0|\mathbf{r}_0+\mathbf{r}_1,t)w_\beta(\mathbf{r}_0|\mathbf{r}_0+\mathbf{r}_1,t)]\rangle, \tag{2.26}$$

$$J^\delta_{2m+1}(\mathbf{R})=2m\nu\langle w^{2(m-1)}w_\delta w_\alpha[\nabla_r^2+\nabla_{r_0}^2]w_\alpha\rangle+\nu\langle w^{2m}[\nabla_r^2+\nabla_{r_0}^2]w_\delta\rangle, \tag{2.27}$$

$$Q^\delta_{2m+1}(\mathbf{R})=2m\langle w^{2(m-1)}w_\delta w_\alpha[f_\alpha(\mathbf{r}_0|\mathbf{r},t)-f_\alpha(\mathbf{r}_0|\mathbf{r}_0,t)]\rangle+\langle w^{2m}[f_\delta(\mathbf{r}_0|\mathbf{r},t)-f_\delta(\mathbf{r}_0|\mathbf{r}_0,t)]\rangle. \tag{2.28}$$

For isotropic turbulence all these vector quantities have obvious scalar counterparts, similar to the one introduced in (2.4). For example,

$$D^{\alpha}_{2m+1}(\mathbf{R})=\frac{R_\alpha}{R}D_{2m+1}(R), \tag{2.29}$$

$$J^{\alpha}_{2m+1}(\mathbf{R})=\frac{R_\alpha}{R}J_{2m+1}(R). \tag{2.30}$$

With these definitions we can rewrite the balance equation (2.25) in the form

$$D_{2m+1}(R)=J_{2m+1}(R)+Q_{2m+1}(R). \tag{2.31}$$

Together with (2.24) we can finally write for n odd or even

$$D_n(R)=J_n(R)+Q_n(R). \tag{2.32}$$

We discuss each term in the balance equation in the following subsections.

C. The terms of the balance equation

1. The interaction term

To understand how to evaluate $D_{2m}(R)$ we begin the discussion by neglecting the effect of the pressure term in the Navier-Stokes equation. This is equivalent to replacing the kernel of the projection operator $P_{\alpha\beta}(r)$ by the unit operator $\delta_{\alpha\beta}\delta(\mathbf{r})$. The effect of this replacement of kernels is to change $D_{2m}(R)$ to

$$D_{2m}(R)=2m\left\langle w^{2(m-1)}w_\alpha w_\gamma\frac{\partial w_\alpha}{\partial r_\gamma}\right\rangle. \tag{2.33}$$

This may be rewritten as

$$D_{2m}(R)=\frac{\partial}{\partial r_\gamma}\langle w_\gamma w^{2m}\rangle=\frac{\partial}{\partial R_\gamma}S^{\gamma}_{2m+1}(\mathbf{R}) \tag{2.34}$$

(neglecting pressure). This expression is relevant for the one-dimensional Burgers equation, since there is no pressure in that case. On the other hand, the Burgers equation describes a compressible flow, and this fact introduces the coefficient $(n+1)/n$ in the right-hand side (RHS) of this expression. For the Navier-Stokes equations we can only use the expression for a rough evaluation of D_{2m}. Notwithstanding, it is exact for the case $m=1$, where it takes the form

$$D_2(R)=\frac{\partial}{\partial R_\alpha}S^{\alpha}_3(\mathbf{R}). \tag{2.35}$$

The deep reason for this simplification in the case $m=1$ is the conservation law (in the absence of viscosity) of the quadratic invariant of the BL equation of motion (2.10), i.e., $\int d\mathbf{r}\mathbf{w}^2[\mathbf{r}_0|\mathbf{r},t]$. $D_2(R)$ is simply the rate of change of $\mathbf{w}^2[\mathbf{r}_0|\mathbf{R},t]$ and therefore must be a pure divergence. None of the higher powers of $\mathbf{w}[\mathbf{r}_0|\mathbf{R},t]$ forms an invariant, and as a consequence none of the higher orders $D_n(R)$ can be written as a pure divergence. On the other hand, we see from Eq. (2.21) that with the full kernel we have two terms that can be expressed in terms of the T tensors:

$$D_{2m}(R)=2m\int d\mathbf{r}_1 P_{\alpha\beta}(\mathbf{r}_1)\frac{\partial}{\partial r_{1\gamma}}[T^{\alpha\beta\gamma}_{2m+1}(\mathbf{R}+\mathbf{r}_1,\mathbf{R}+\mathbf{r}_1,\mathbf{R})-T^{\alpha\beta\gamma}_{2m+1}(\mathbf{r}_1,\mathbf{r}_1,\mathbf{R})]. \tag{2.36}$$

This is the final form of $D_{2m}(R)$.

Following the same steps of analysis we find the final expression for $\mathbf{D}_{2m+1}(\mathbf{R})$:

$$\begin{aligned}D^{\delta}_{2m+1}(\mathbf{R})=2m&\int d\mathbf{r}_1 P_{\alpha\beta}(\mathbf{r}_1)\frac{\partial}{\partial r_{1\gamma}}\{T^{\alpha\beta\gamma\delta}_{2m+2}(\mathbf{R}+\mathbf{r}_1,\mathbf{R}+\mathbf{r}_1,\mathbf{R})-T^{\alpha\beta\gamma\delta}_{2m+2}(\mathbf{r}_1,\mathbf{r}_1,\mathbf{R})\}\\&+\int d\mathbf{r}_1 P_{\delta\beta}(\mathbf{r}_1)\frac{\partial}{\partial r_{1\gamma}}\{T^{\beta\gamma}_{2m+2}(\mathbf{R}+\mathbf{r}_1,\mathbf{R}+\mathbf{r}_1,\mathbf{R})-T^{\beta\gamma}_{2m+2}(\mathbf{r}_1,\mathbf{r}_1,\mathbf{R})\}.\end{aligned} \tag{2.37}$$

The naive evaluation of every term in Eq. (2.36) is given by (2.34). However, this evaluation is only acceptable under two assumptions: (i) that the integral converges, and (ii) that there are no cancellations between the terms with opposite signs in Eq. (2.36). The analysis of convergence requires understanding the asymptotic properties of the T correlators. Similar properties will determine the evaluation of J_{2m} as will be seen next. For that reason we will devote the next sections to questions of asymptotics and fusion rules for the n-point correlation function of velocity differences. We will learn that the integral in Eq. (2.36) indeed converges, but on the other hand cancellations are not excluded and are one possible source of multiscaling in turbulence. In fact, such a cancellation is one of the mechanisms of multiscaling that we can identify.

2. The dissipation term

Starting with (2.22) we first use the fact that for simultaneous correlations we can use the Eulerian differences $\delta\mathbf{u}$ instead of the BL velocity differences. Second, we use the symmetry with respect to exchange of $\mathbf{r}$ and $\mathbf{r}_0$ to write the expression with twice the Laplacian with respect to $\mathbf{r}_0$ only, instead of the sum of Laplacians. Lastly we use translational invariance to move one of the gradients around. We find

$$J_{2m}(R)\equiv -4m\nu\left\{\left\langle |\delta\mathbf{u}(\mathbf{r}_0|\mathbf{R})|^{2(m-1)}\left[\frac{\partial}{\partial r_{0\beta}}u_\alpha(\mathbf{r}_0)\right]^2\right\rangle + 2(m-1)\left\langle |\delta\mathbf{u}(\mathbf{r}_0|\mathbf{R})|^{2(m-2)}\delta u_\alpha(\mathbf{r}_0|\mathbf{R})\,\delta u_\gamma(\mathbf{r}_0|\mathbf{R})\frac{\partial}{\partial r_{0\beta}}u_\gamma(\mathbf{r}_0)\frac{\partial}{\partial r_{0\beta}}u_\alpha(\mathbf{r}_0)\right\rangle\right\}. \tag{2.38}$$

To relate this quantity to the tensors T defined in Eqs. (2.6)–(2.8) we write the derivative as the limit of velocity differences:

$$\frac{\partial}{\partial r_{0\beta}}u_\alpha(\mathbf{r}_0)\equiv\lim_{d_\beta\to 0}\frac{u_\alpha(\mathbf{r}_0+d_\beta\mathbf{e}_\beta)-u_\alpha(\mathbf{r}_0)}{d_\beta}, \tag{2.39}$$

where $\mathbf{e}_\beta$ is the unit vector in the β direction. With this in mind the expression for J_{2m} is

$$J_{2m}(R)=-4m\nu\lim_{d_\beta\to 0}\frac{1}{d_\beta^2}[T_{2m}^{\alpha\alpha}(d_\beta\mathbf{e}_\beta,d_\beta\mathbf{e}_\beta,\mathbf{R}) + 2(m-1)T_{2m}^{\alpha\gamma\alpha\gamma}(d_\beta\mathbf{e}_\beta,d_\beta\mathbf{e}_\beta,\mathbf{R})]. \tag{2.40}$$

One should understand that a summation over α, β, and γ is implied as usual. Note that for $d_\beta\ll\eta$ the velocity field is expected to be smooth, and both T functions become proportional to d_β^2, canceling this factor in the denominator. We will not have a dependence of the limit on the direction of the vector $\mathbf{d}\equiv d_\beta\mathbf{e}_\beta$.

It can be seen that the evaluation of $J_{2m}(R)$ again requires elucidation of the asymptotic properties of the correlation functions including the rules of coalescence of groups of points. In paper I we proved the property of locality that means that the coalescence itself is regular. However, we have here differential operators on coalescing points and we need to consider not only leading behaviors but also next order properties. This is done in Sec. V.

The quantities $J_{2m+1}^\alpha(\mathbf{R})$ can be expressed in terms of the third and fifth rank T tensors, but we avoid displaying the result since we do not use it explicitly.

Finally we need to discuss the forcing terms $Q_{2m}(R)$ and $Q_{2m+1}^\alpha(\mathbf{R})$. This is the topic of the next subsection.

3. The forcing term

In this subsection we show that the forcing term can be neglected in the inertial range of scales. The reader who finds this statement believable can skip this subsection. To discuss the forcing terms it is useful to introduce a higher order Green's function according to

$$\mathcal{G}_{2m-1,1}^{\alpha\beta}(\mathbf{r}_0|x,x')\equiv\left\langle\frac{\delta w^{2(m-1)}w_\alpha}{\delta\tilde f_\beta(\mathbf{r}_0|x')}\right\rangle. \tag{2.41}$$

We remind the reader that $x=(\mathbf{r},t)$ and that according to our convention we can omit the argument $(\mathbf{r}_0|x)$ in the function $\mathbf{w}$.

When the statistics of the random forcing is Gaussian we can write $Q_{2m}(R)$ of Eq. (2.22) as

$$Q_{2m}(R)=\int d\mathbf{r}'dt'\,\mathcal{G}_{2m-1,1}^{\alpha\beta}(\mathbf{r}_0|x,x')[D_{\alpha\beta}(\mathbf{r}_0|\mathbf{r}',\mathbf{r},t'-t) - D_{\alpha\beta}(\mathbf{r}_0|\mathbf{r}',\mathbf{r}_0,t'-t)]. \tag{2.42}$$

Here, as usual, $\mathbf{R}=\mathbf{r}-\mathbf{r}_0$ and $D_{\alpha\beta}(\mathbf{r}_0|x,x')$ is the correlator of $\tilde f_{\alpha(x)}$ and $\tilde f_{\beta(x)}$.

We are going to estimate $Q_{2m}(R)$ by taking first a δ-correlated forcing,

$$D_{\alpha\beta}(\mathbf{r}_0|x,x')=D_{\alpha\beta}(\mathbf{r}-\mathbf{r}')\,\delta(t-t'). \tag{2.43}$$

The consideration of the effect of finite correlation time is deferred to the end. Using (2.43) Eq. (2.42) simplifies to

$$Q_{2m}(R)=\int d\mathbf{r}'\,\mathcal{G}_{2m-1,1}^{\alpha\beta}(\mathbf{r}_0|\mathbf{r},\mathbf{r}',0)[D_{\alpha\beta}(\mathbf{r}'-\mathbf{r}) - D_{\alpha\beta}(\mathbf{r}'-\mathbf{r}_0)]. \tag{2.44}$$

Because of the δ functions we have lost the time integration and we have the zero-time Green's function, which is not dressed by the interaction (and see paper I for an explicit demonstration). Using the chain rule of differentiation in (2.41) we get

$$\mathcal{G}_{2m-1,1}^{\alpha\beta}(\mathbf{r}_0|x,x')=\left\langle w^{2(m-1)}\frac{\delta w_\alpha}{\delta\tilde f_\beta(\mathbf{r}_0|x')}\right\rangle + 2(m-1)\times\left\langle w^{2(m-2)}w_\alpha w_\gamma\frac{\delta w_\gamma}{\delta\tilde f_\beta(\mathbf{r}_0|x')}\right\rangle. \tag{2.45}$$

Next we recall that at time $t=0$ the unaveraged response $\delta w/\delta\tilde f$ is uncorrelated with the velocity field since any interaction involves a vertex with time integration between 0 and t. Accordingly we can decouple the response in (2.45) and write

$$\mathcal{G}_{2m-1,1}^{\alpha\beta}(\mathbf{r}_0|x,x')=\mathcal{G}_{\alpha\beta}^0(\mathbf{r}_0|\mathbf{r},\mathbf{r}')\mathring{S}_{2(m-1)}(R)+2(m-1)\mathcal{G}_{\gamma\beta}^0(\mathbf{r}_0|\mathbf{r},\mathbf{r}')S_{2(m-1)}^{\alpha\gamma}(R), \tag{2.46}$$

where $\mathcal{G}^0$ is the bare Green's function, which was defined and computed in paper I, Secs. II and III. We proceed to evaluate the order of magnitude of Q_{2m} by substituting the last equation in (2.44). Suppressing vector indices, we evaluate

$$Q_{2m}(R)\simeq m(2m-1)S_{2(m-1)}(R)Q_2(R), \tag{2.47}$$

where

$$Q_2(R)=\int d\mathbf{r}'\,\mathscr{G}^0(\mathbf{r}_0|\mathbf{r},\mathbf{r}',0)[D(\mathbf{r}'-\mathbf{r})-D(\mathbf{r}'-\mathbf{r}_0)]. \tag{2.48}$$

We can estimate Q_2 by recalling that $D(R)$ has a characteristic scale L (which is the outer scale of turbulence). For $R\ll L$ we expand $D(R)$ in R:

$$D(R)=D(0)+D''R^2/2,\quad D''\simeq D(0)/L^2. \tag{2.49}$$

In its turn $D(0)$ is about the rate of energy input, and for stationary turbulence $D(0)\simeq\bar{\epsilon}$, the rate of energy dissipation. Finally we estimate

$$D(R)-D(0)\simeq\bar{\epsilon}(R/L)^2. \tag{2.50}$$

Together with the evaluation of G^0 that was presented in paper I, Sec. III B we evaluate Q_2 as

$$Q_2(R)\sim\frac{\bar{\epsilon}}{L^2}\int d\mathbf{r}'\,\frac{|\mathbf{R}-\mathbf{r}'|^2-r'^2}{|\mathbf{R}-\mathbf{r}'|^3-r'^3}. \tag{2.51}$$

The integral can be evaluated by introducing the ultraviolet cutoff at the viscous scale η:

$$Q_2\sim\bar{\epsilon}\left(\frac{R}{L}\right)^2\ln\left(\frac{R}{\eta}\right). \tag{2.52}$$

Substituting in (2.47) and omitting numerical factors we end up with

$$Q_{2m}(R)\sim\bar{\epsilon}\left(\frac{R}{L}\right)^2 S_{2(m-1)}(R)\ln\left(\frac{R}{\eta}\right). \tag{2.53}$$

We are now in a position to compare Q_{2m} with the interaction term D_{2m} given in (2.33). For K41 scaling and δ-correlated forcing we have

$$\frac{Q_{2m}}{D_{2m}}\sim\left(\frac{R}{L}\right)^2\ln\left(\frac{R}{\eta}\right). \tag{2.54}$$

It should be noted that the logarithm in this equation is a direct result of our use of δ correlated forcing. This choice brought in the zero-time Green's function with its inverse cubic R dependence, which led to the logarithm. Any realistic forcing would be integrated against the finite time response, which is less singular than the zero time function. We thus assert at this point that a more detailed analysis should reveal that Q_{2m} is negligible compared to D_{2m} in the core of the inertial interval. The power law $(R/L)^2$ for the ratio of these quantities is appropriate for K41 scaling, and the exponent may be slightly different for non-K41 exponents. At any rate we are satisfied that for $R\ll L$ the forcing term is negligible compared to the transfer term.

III. THE ANOMALOUS EXPONENT ASSOCIATED WITH PAIR COALESCENCE

In this section we begin the exploration of the ultraviolet properties of n-point correlation functions with the aim of computing J_n and D_n of the previous section. To achieve this we examine first a second-order Green's function of the type introduced in paper II and whose ultraviolet properties are characterized by an anomalous exponent Δ. We will prove that these ultraviolet properties are shared by the second order structure function, and that Δ attains the critical value $\Delta=2-\zeta_2$. Although this statement was made already in paper II, Sec. V B, we discuss it here in full detail because of its crucial importance for the structure of the theory of turbulence, and in particular in determining also the ultraviolet properties of the quantities appearing in the balance equations (2.24) and (2.25). We begin with the four-point Green's functions. The analysis of this section will allow us already to evaluate the correlation function of the dissipation field (1.4). The strategy of this section is first to introduce the needed many-point Green's functions, then to examine and classify their diagrammatic representation, and last to resum the diagrammatic series to obtain exact integral equations for these quantities. The exact equations will allow us to find nonperturbative solutions.

A. Many-point Green's functions

1. Definitions

Consider the nonlinear Green's functions $\mathscr{G}_{m,n}$, which are the response of the product of m BL velocity differences to n perturbations. In particular,

$$\mathscr{G}_{2,1}^{\alpha\beta\gamma}(\mathbf{r}_0|x_1,x_2,x_3)=\left\langle\frac{\delta[w_\alpha(\mathbf{r}_0|x_1)w_\beta(\mathbf{r}_0|x_2)]}{\delta h_\gamma(x_3)}\right\rangle, \tag{3.1}$$

$$\mathscr{G}_{1,2}^{\alpha\beta\gamma}(\mathbf{r}_0|x_1,x_2,x_3)=\left\langle\frac{\delta^2 w_\alpha(\mathbf{r}_0|x_1)}{\delta h_\beta(\mathbf{r}_0|x_2)\,\delta h_\gamma(x_3)}\right\rangle, \tag{3.2}$$

$$\mathscr{G}_{2,2}^{\alpha\beta\gamma\delta}(\mathbf{r}_0|x_1,x_2,x_3,x_4)=\left\langle\frac{\delta^2[w_\alpha(\mathbf{r}_0|x_1)w_\beta(\mathbf{r}_0|x_2)]}{\delta h_\gamma(x_3)\,\delta h_\delta(x_4)}\right\rangle, \tag{3.3}$$

$$\mathscr{G}_{3,1}^{\alpha\beta\gamma\delta}(\mathbf{r}_0|x_1,x_2,x_3,x_4)=\left\langle\frac{\delta[w_\alpha(\mathbf{r}_0|x_1)w_\beta(\mathbf{r}_0|x_2)w_\gamma(x_3)]}{\delta h_\delta(x_4)}\right\rangle. \tag{3.4}$$

Note that these are different from the nonlinear Greens' function G_2 that was dealt with extensively in paper II,

$$G_2^{\alpha\beta\gamma\delta}(\mathbf{r}_0|x_1,x_2,x_3,x_4)=\left\langle\frac{\delta w_\alpha(\mathbf{r}_0|x_1)}{\delta h_\gamma(x_3)}\,\frac{\delta w_\beta(\mathbf{r}_0|x_2)}{\delta h_\delta(x_4)}\right\rangle. \tag{3.5}$$

One can see that the relation between these four-point Green's functions follows from the chain rule of differentiation and is

$$\begin{aligned}\mathscr{G}_{2,2}^{\alpha\beta\gamma\delta}(\mathbf{r}_0|x_1,x_2,x_3,x_4)=&\,G_2^{\alpha\beta\gamma\delta}(\mathbf{r}_0|x_1,x_2,x_3,x_4)\\&+G_2^{\alpha\beta\delta\gamma}(\mathbf{r}_0|x_1,x_2,x_4,x_3)\\&+\left\langle\frac{w_\alpha(\mathbf{r}_0|x_1)\,\delta^2 w_\beta(\mathbf{r}_0|x_2)}{\delta h_\gamma(x_3)\,\delta h_\delta(x_4)}\right\rangle\\&+\left\langle\frac{w_\beta(\mathbf{r}_0|x_2)\,\delta^2 w_\alpha(\mathbf{r}_0|x_1)}{\delta h_\gamma(x_3)\,\delta h_\delta(x_4)}\right\rangle.\end{aligned} \tag{3.6}$$

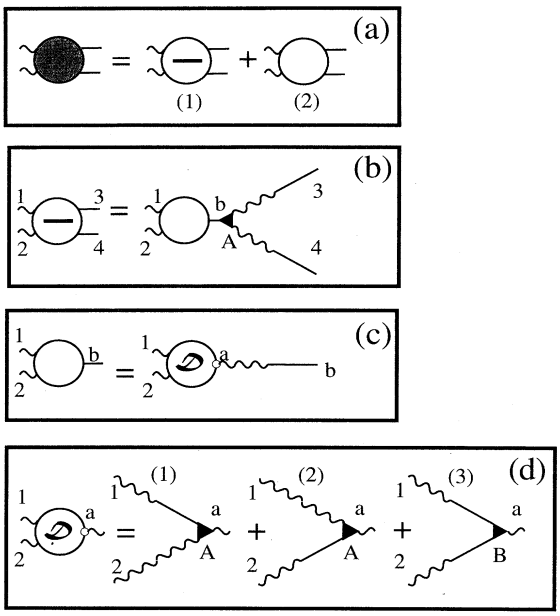

FIG. 1. Diagrammatic representation of the four-point Green's function $\mathscr{G}_{2,2}$ defined by Eq. (3.3). (a) $\mathscr{G}_{2,2}$ as a sum of weakly linked contributions $\mathscr{G}^{\rm wl}_{2,2}$ [shown in (b)–(d)] and strongly linked contribution $\mathscr{G}^{\rm sl}_{2,2}$ (shown on Fig. 2). (b) $\mathscr{G}^{\rm wl}_{2,2}$ is presented in terms of the three-point Green's function $\mathscr{G}_{2,1}$, defined by Eq. (3.1), and the dressed vertex A. (c) and (d) give the diagrammatic representation of $\mathscr{G}_{2,1}$ in terms of the propagators G and F_2 and the dressed vertices A and B. For the diagrammatic expansion of the dressed vertices A, B, and C; see Fig. 7 of paper II. Note the new notation of an empty little circle in the object $\mathscr{D}$. This circle designates a vertex that can be either bare or dressed.

In order to analyze the properties of the functions $\mathscr{G}_{m,n}$ we will explore their diagrammatic representation.

2. Diagrammatic representation

In Sec. III A of paper II it was explained in detail how to produce the diagrammatic representation of G_2. Very similar steps lead to the diagrams for $\mathscr{G}_{2,2}$, which are shown in Fig. 1. Of course, due to (3.6) all the diagrams of G_2 appear also in the representation of $\mathscr{G}_{2,2}$. These common diagrams all have two principal paths made of Green's functions as explained in paper II. In $\mathscr{G}_{2,2}$ there are contributions coming from the last two terms in (3.6). To understand the structure of these new diagrams note that every diagram representing $\delta^2 w_1 / \delta h_3 \delta h_4$ has a principal path of Green's functions that starts with coordinate x_1 or x_2, which splits at some point into two principal paths made of Green's functions ending up with the coordinates x_3, x_4. The field w_2 itself is another tree of the type appearing in Fig. 3 of paper II. Upon multiplying these trees and averaging over the Gaussian ensemble of forces we get diagrams that are ready to be resummed. One set of diagrams that appears are those that have a bridge made of a single Green's function connecting the "left" part of the diagram (coordinates $\mathbf{r}_1, \mathbf{r}_2$) to the "right" part of the diagram (coordinates $\mathbf{r}_3, \mathbf{r}_4$). By necessity this Green's function belongs to the principal path of the diagram, which is made of Green's functions. We note that a bridge made of a single propagator may appear only once. A second single propagator bridge makes the diagram "one-eddy reducible," and such diagrams have already been line resummed; see paper 0 for more details. Every decoration to the left of the bridge may be resummed into a dressed vertex on the left, and every decoration on the right of the bridge may be resummed into a dressed vertex on the right. The fully resummed series of weakly linked (via one-propagator bridge) diagrams, which we denote as $\mathscr{G}^{\rm wl}_{2,2}$, contains exactly the two diagrams that are shown in Figs. 1(b)–1(d).

The reader's attention should be drawn to the weakly linked diagrams that have appeared here. It will turn out that these diagrams play a very important role in the mechanism that we propose for anomalous scaling in turbulence. For that reason we pause for a moment to discuss the topological structure of these diagrams in more detail. By construction the bridge between points (1,2) and (3,4) in the diagrams for $\mathscr{G}^{\rm wl}_{2,2}(\mathbf{r}_0|x_1,x_2,x_3,x_4)$ can consist of a Green's function but not of a correlator. In Fig. 1(c) the coordinates of the Green's function are denoted by x_a, x_b. On the two sides of the a-b bridge there exist three-point objects. These objects have an exact resummed form in terms of the dressed vertices A and B, which were introduced briefly in paper I. Note that we have a freedom in the diagrammatic representation as to whether to include the bridge itself together with the object on the right or on the left. In the former case the resulting object on the right is $\mathscr{G}_{1,2}(\mathbf{r}_0|x_a,x_3,x_4)$, which was defined in (3.2). In the latter case, which is the convention that we choose, see Fig. 1(b), the resulting object on the left side is $\mathscr{G}_{2,1}(\mathbf{r}_0|x_1,x_2,x_b)$, which is defined in (3.1). In order to display the bridge a-b explicitly we introduce in Fig. 1(c) an object denoted as $\mathscr{D}(\mathbf{r}_0|x_1,x_2,x_a)$. This object has two "entries" 1 and 2, starting with propagators and one "exit" denoted x_a, which ends with a vertex, Fig. 1(d). We will use an empty small circle to denote the position of a vertex. This is done to distinguish a vertex from a propagator leg.

Next, as explained in paper II, we need to identify two-eddy reducible and two-eddy irreducible diagrams. The first type are diagrams that can be split into a left and a right part by cutting two propagators. For G_2 these propagators can only be Green's functions. This is the cross section denoted by a in Fig. 2. In the present case we can also have cross sections of type b with one Green's function and one propagator. There cannot be cross sections with two correlators because we always have at least one principal path of Green's functions that connects the left part of the diagrams to its right part. Finally we can have a cross section of type c in which two Green's functions appear in opposite orientations.

In summary, the structure of the diagrammatic series can be described as follows: we get ladder diagrams that have alternating Green's functions and double correlators in any possible order, as long as there is at least one Green's function between two rungs that carries the principal path. The ladder diagrams can have alternating rungs of three types, depending on the type of propagators preceding the rung. The three types of rungs are sums of two-eddy irreducible diagrams that are denoted $\Sigma_{(1,3)}$, $\Sigma_{(2,2)}$, and $\Sigma_{(3,1)}$, respectively. Graphically they are represented by a dashed bar, an empty bar, and doubly dashed bar, respectively. The first one has three straight tails and one wavy tail, the second one has

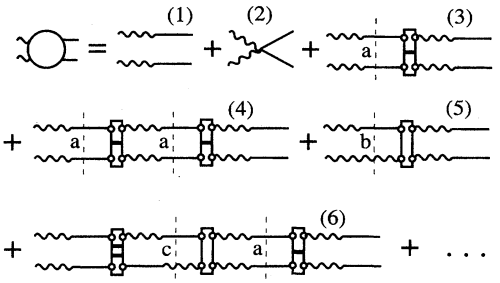

FIG. 2. The diagrammatic presentation of the strongly linked contribution $\mathscr{G}^{\rm sl}_{2,2}$ to the four-point Green's function $\mathscr{G}_{2,2}$ (see Fig. 1). Diagrams (1) and (2) are the Gaussian decomposition of $\mathscr{G}^{\rm sl}_{2,2}$, diagrams (3) and (5) are ladders with one rung (of two types), and diagrams (3) and (6) are the ladders with two and three rungs, respectively. In contrast to the expansion in Fig. 9 of paper II for G_2, here one has rungs of three types. These are $\Sigma_{3,1}$ as in diagram (5), $\Sigma_{2,2}$ as in diagrams (3) and (4), and rung $\Sigma_{1,3}$ as the first rung in diagram (6). The diagrammatic expansion of $\Sigma_{2,2}$ is shown in Fig. 3, and the expansion of $\Sigma_{3,1}$ and $\Sigma_{1,3}$ in Fig. 4. The exact resummation of this series is shown in Fig. 5.

two straight and two wavy tails, and the last has three wavy and one straight tail. The series for $\Sigma_{(n,m)}$ are shown in Figs. 3 and 4. Figure 2 shows the diagrams for $\Sigma_{(2,2)}$. This series is composed of all the diagrams in Fig. 10(a) of paper II (and diagrams 1, 2, and 5 in Fig. 3 are examples of those) in addition to new diagrams like diagrams 3 and 4 in Fig. 3. All the old diagrams have a horizontal principal cross section that cuts through correlators only. The new diagrams contain the split in the principal path, and the principal cross section through correlators turns up or down by 90°. The series for the two other two-eddy irreducible mass operator $\Sigma_{(1,3)}$ and $\Sigma_{(3,1)}$ are shown in Fig. 4. The diagrams in these series have no principal cross section that cuts through correlators only.

3. *Resummation of the strongly linked contributions*

As in the case of the ladder diagrams of G_2 we can resum also in the case of $\mathscr{G}^{\rm sl}_{2,2}$ all the ladder diagrams into integral

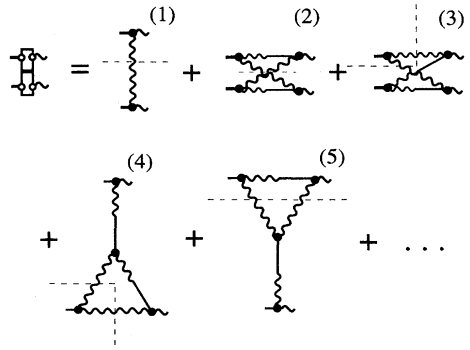

FIG. 3. Diagrammatic expansion for the mass operator $\Sigma_{2,2}$, which is found in the expansion of $\mathscr{G}^{\rm sl}_{2,2}$ shown in Fig. 2. This mass operator is an important element in the system of equations for $\mathscr{G}^{\rm sl}_{2,2}$ and $\mathscr{G}^{\rm sl}_{3,1}$ shown in Fig. 5. The principal cross sections are shown as dashed lines.

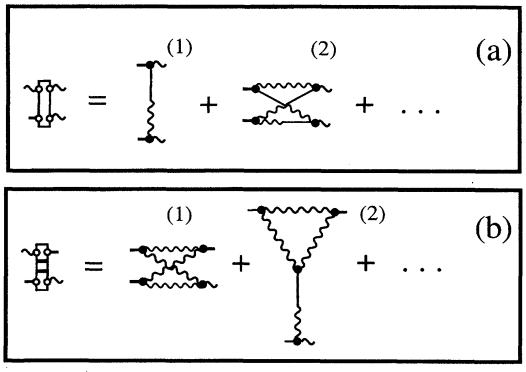

FIG. 4. Diagrammatic expansions of the mass operator $\Sigma_{3,1}$ (a) and $\Sigma_{1,3}$ (b), which appear in the expansion of $\mathscr{G}^{\rm sl}_{2,2}$ shown in Fig. 2. These mass operators are the essential elements in the equations shown in Fig. 5.

equations. The resummed ladders are shown in Fig. 5. The diagrammatic notation of $\mathscr{G}^{\rm sl}_{2,2}$ is an empty circle with two wavy and two straight lines. It has three different types of contributions. First come the reducible contributions that we denote by $\mathscr{G}^{(0)}_{2,2}$ and are represented by the unlinked diagrams (1) and (2) of Fig. 2. The first two ladders (3) and (4) in Fig. 2 are identical to the RHS of the resummed equation for G_2. The next term on the RHS in Fig. 2 is new. The resummation of the ladders is shown in Fig. 5. On the RHS of the diagrammatic equation we find a Green's function that is defined in (3.4) as $\mathscr{G}_{3,1}$ and whose graphic notation has a crossed circle with three wavy and one straight tails. This object is again resummed in terms of itself and $\mathscr{G}_{2,2}$ as shown in Fig. 5(b).

In conclusion we learn that the four-point Green's functions $\mathscr{G}_{m,n}$ satisfy equations that contain linear operators act-

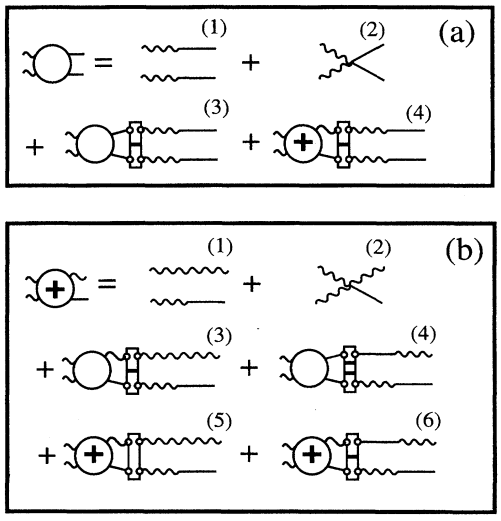

FIG. 5. The exact system of equations for the strongly linked contributions to $\mathscr{G}_{2,2}$ (a) and $\mathscr{G}_{3,1}$ (b) in terms of the propagators G and F_2 and the mass operators $\Sigma_{3,1}$, $\Sigma_{2,2}$ and $\Sigma_{1,3}$. The first terms in the expansion of $\Sigma_{m,n}$ are shown in Figs. 3 and 4. This system results from the exact resummation of ladder diagrams.

ing on $\mathscr{G}_{m,n}$ and inhomogeneous terms that are products of G's and the weakly linked contributions. To be sure, the linear operators are themselves functionals of $\mathscr{G}_{m,n}$, so that our equations are in fact nonlinear. If we expand the solutions of these inhomogeneous nonlinear equations around the inhomogeneous terms we generate back the initial diagrammatic expansion. However, now we can also explore the "*homogeneous*" solutions of these equation that are obtained by discarding the inhomogeneous terms. Such solutions, if they exist, are manifestly nonperturbative effects. We will need to show *a posteriori* that these nonperturbative solutions are much larger than the solutions that can be found from perturbative analysis. Indeed, in paper II it was shown in detail that G_2 has such a nonperturbative homogeneous solution with the following property: when the first two coordinates r_1 and r_2 are of the same order (say r) and much smaller than the last two coordinates r_3 and r_4 (which are of the order of R) then

$$\nabla_r^2 G_2(r,r,R,R) \sim r^{-\Delta} \quad \text{for } R \gg r. \tag{3.7}$$

Since the same terms appear in the equation for $\mathscr{G}_{2,2}$ we know that such a divergence (with $r \to 0$) must appear also in all $\mathscr{G}_{n,m}$. (This of course hinges on the assumption that the terms in Fig. 5 do not contribute an exact cancellation; in view of their different nature we judge this possibility unlikely.) These terms may have a stronger or a weaker divergence, and we turn now therefore to an exact calculation of the value of Δ.

B. Calculation of Δ

In order to evaluate Δ we establish a fundamental identity,

$$\frac{\delta F_{\alpha\beta}(\mathbf{r}_0|x_1,x_2)}{\delta D_{\gamma\delta}(x_3,x_4)} = \mathscr{G}_{2,2}^{\alpha\beta\gamma\delta}(\mathbf{r}_0|x_1,x_2,x_3,x_4), \tag{3.8}$$

where the covariance D is the correlation of the perturbations,

$$D_{\gamma\delta}(x_3,x_4) = \langle h_\gamma(x_3) h_\delta(x_4) \rangle. \tag{3.9}$$

The identity is proved most easily using the path integral formulation as reviewed in paper I. In terms of the functional $\mathscr{Z}(\mathbf{l},\mathbf{m})$ of Eq. (I-3.12) the second order Green's function is

$$\mathscr{G}_{2,2}^{\alpha\beta\gamma\delta}(\mathbf{r}_0|x_1,x_2,x_3,x_4) = -\langle w_\alpha(\mathbf{r}_0|x_1) w_\beta(\mathbf{r}_0|x_2) p_\gamma(x_3) p_\delta(x_4) \rangle. \tag{3.10}$$

On the other hand we see from Eq. (I-3.14) that the derivative with respect to $D_{\alpha\beta}$ brings down $ip_\alpha p_\beta$:

$$\frac{\delta I_0}{\delta D_{\gamma\delta}(x-y)} = i p_\gamma(x) p_\delta(y). \tag{3.11}$$

This means that the functional derivative of $\langle w_\alpha w_\beta \rangle$ with respect to $D_{\gamma\delta}$ is precisely the RHS of (3.10). This is the proof of the identity.

Rewrite now the identity in the form

$$\delta F_{\alpha\beta}(\mathbf{r}_0|x_1,x_2) = \int dx_3 dx_4 \mathscr{G}_{2,2}^{\alpha\beta\gamma\delta}(\mathbf{r}_0|x_1,x_2,x_3,x_4) \times \delta D_{\gamma\delta}(x_3,x_4). \tag{3.12}$$

In this form this is a relation of the response δF in the velocity correlator F to a variation in the correlator of the random forcing δD. It is clear now that if the random forcing is limited to scales $r_3, r_4 \gg r_1, r_2$, the existence of flux equilibrium with a scaling solution for $F_{\alpha\beta}(\mathbf{r}_0|x_1,x_2)$ means that the variation $\delta F_{\alpha\beta}(\mathbf{r}_0|x_1,x_2)$ must be proportional to $F_{\alpha\beta}(\mathbf{r}_0|x_1,x_2)$ itself. We can have a change in the amplitude but not in the functional form:

$$\delta F_{\alpha\beta}(\mathbf{r}_0|x_1,x_2) \propto F_{\alpha\beta}(\mathbf{r}_0|x_1,x_2) \quad \text{for } r_1, r_2 \ll r_3, r_4. \tag{3.13}$$

To understand what are the requirements of the variation $\delta D_{\gamma\delta}(x_3,x_4)$ that guarantee the validity of the universal behavior (3.13) let us write again the Wyld equation (II-2.9). We will use economic notation, such that the vector index carries implicitly also the position coordinate. Repeated indices must be summed upon and the convention is that this sum also requires integration over the intermediate position coordinates. This convention allows us to write the Wyld equation as

$$F_{\alpha\beta} = G_{\alpha\gamma}[D_{\gamma\delta} + \Phi_{\gamma\delta}] G_{\beta\delta}. \tag{3.14}$$

The variation $\delta D_{\gamma\delta}$ causes a variation in F. In our convention

$$F_{\alpha\beta} + \delta F_{\alpha\beta} = G_{\alpha\gamma}[D_{\gamma\delta} + \delta D_{\gamma\delta} + \Phi_{\gamma\delta}] G_{\beta\delta}. \tag{3.15}$$

Next note that $\Phi_{\gamma\delta}(\mathbf{r}_0|x_a,x_b)$ can be exactly expressed as a second derivative of the four-point correlation function $F_4(x_a,x_a,x_b,x_b)$; cf. Eq. (I-4.5). Consequently

$$\Phi_{\gamma\delta}(\mathbf{r}_0|x_a,x_b) \sim r_{ab}^{\zeta_4 - 2}. \tag{3.16}$$

We know that ζ_4 is expected to be considerably smaller than 2. (The K41 estimate is $\zeta_4 = 4/3$, whereas experimentally one finds $\zeta_4 \sim 1.2$.) Thus $\Phi_{\gamma\delta}(\mathbf{r}_0|x_a,x_b)$ is *growing* when the coordinates become smaller, whereas $\delta D_{\gamma\delta}$ is restricted to the large scales and is *decaying* for smaller coordinates. We expect therefore that δF will be proportional to F and the constant of proportionality is determined by the boundary conditions at large scales where both D and δD are not negligible.

For future reference we should note at this point that the proportionality of $\delta F^{\alpha\beta}$ and $F^{\alpha\beta}$ is not restricted only to their scaling exponents. In fact the two quantities have the same tensor structure. In other words they are the same function of $\mathbf{r}_1 - \mathbf{r}_0$ and $\mathbf{r}_2 - \mathbf{r}_0$ up to constants that are independent of the tensor indices. To complete the argument choose now $t_1 = t_2$. Next notice the fact that

$$\nabla_1 \cdot \nabla_2 F_{\alpha\beta}(\mathbf{r}_0|\mathbf{r}_1,\mathbf{r}_2) \propto r_{12}^{\zeta_2 - 2}. \tag{3.17}$$

Now restrict $\delta D_{\gamma\delta}(x_3,x_4)$ to $r_3, r_4 \sim R \gg r_1, r_2$. Applying the operator $\nabla_1 \cdot \nabla_2$ to (3.12) we conclude that

$$\nabla_1 \cdot \nabla_2 \mathscr{G}_{2,2}^{\alpha\beta\gamma\delta}(\mathbf{r}_0|r_1,r_2,x_3,x_4) \propto r_{12}^{\zeta_2 - 2}. \tag{3.18}$$

Note that the RHS is a function of r_{12} only; the reason for this is that under the derivatives the dependence on r_0 disappears. Accordingly the restriction of validity of this result is not necessarily $r_1, r_2 \ll R$ but just $r_{12} \ll R$. Comparing with (3.7) we reach the central result of this section:

$$\Delta = 2 - \zeta_2 . \tag{3.19}$$

Finally we can argue that the application of the operator $\nabla_1 \cdot \nabla_2$ to $\mathscr{G}_{3,1}$ will give rise to the same exponent Δ as in (3.18). To see this apply the operator to the two equations in Fig. 5. Suppose that the divergence associated with $\mathscr{G}_{3,1}$ is stronger than Δ. This will immediately force the divergence of the left-hand side of Fig. 5(a) to be stronger than Δ, in contradiction with our exact result. In the same manner the divergence of $\nabla_1 \cdot \nabla_2 \mathscr{G}_{3,1}$ cannot be weaker than Δ due to the equation in Fig. 5(b). We thus conclude that also

$$\nabla_1 \cdot \nabla_2 \mathscr{G}^{\alpha\beta\gamma\delta}_{3,1}(\mathbf{r}_0 | r_1, r_2, x_3, x_4) \propto r_{12}^{\zeta_2 - 2} . \tag{3.20}$$

C. Three-point objects and the weakly linked inhomogeneous contributions

Equation (3.19) was derived by neglecting the inhomogeneous part of the equation for $\mathscr{G}$. In order to be sure that the inhomogeneous part is not important we need to evaluate now the weakly linked contributions and compare them with (3.18) and (3.20). We are not going to perform the evaluation with the same care as we did in the computation of Δ. All that we need is to show that these terms are negligibly small. We will show this by assuming that the diagrams have the property of rigidity that was demonstrated in paper II order by order. This will be sufficient since we will be able to show that there exists a large gap in the value of the scaling exponents of the homogeneous and the inhomogeneous terms. Such a large gap is not expected to be swamped by nonperturbative effects.

To prepare for this evaluation we need first the diagrammatic representation of three-point objects. These are the three-point correlator F_3, and the Green's functions $\mathscr{G}_{2,1}$ and $\mathscr{G}_{1,2}$. All the three-point objects can be represented with the help of the three types of dressed vertices, which were denoted in paper II as A, B, and C, respectively; see paper II, Fig. 7. We remind the reader that vertex A is a junction of one straight and two wavy lines, vertex B is the junction of two straight and one wavy line, whereas vertex C is the junction of three straight lines. The diagrammatic representation of the triple correlation function F_3 in terms of these vertices is shown in Fig. 7 of paper II, and is reproduced in more compact form in Figs. 6(b) and 6(c). In the same manner the Green's function $\mathscr{G}_{2,1}$ is represented here in Fig. 1(c).

Consider now the weakly linked diagrams for $\mathscr{G}_{2,2}$, which are resummed into the form shown in the diagram in Fig. 1(b). In the limit of $r_1 \sim r_2 \sim r \to 0$ and $r_3 \sim r_4 \sim R$, rigidity means that the integral over r_b contributes mostly in the region $r_b \sim R$. We thus need to understand the r dependence of $\mathscr{G}_{2,1}(\mathbf{r}_0 | x_1, x_2, x_b)$ in the asymptotic situation $r_1, r_2 \ll R$. Looking at Figs. 1(c) and 1(d) we see that due to rigidity the vertices A and B will contribute mostly in the region $r_a \sim r$. In K41 scaling the exponent of r is found by noticing that the correlator contributes r^{ζ_2}, and the Green's

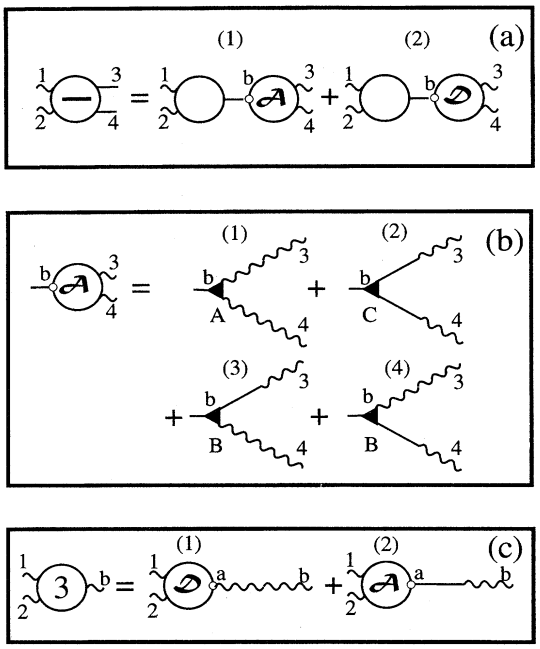

FIG. 6. Diagrammatic representation of the weakly linked contributions to the four-point correlation function F_4. (a) A weakly linked contribution to $F_4(\mathbf{r}_0 | x_1, x_2, x_3, x_4)$ in which a one-propagator bridge is placed between the (1,2) pair and the (3,4) pairs of legs. One has two more similar weakly linked contributions with the bridge connecting the pairs (1,3) with (2,4) and (1,4) with (2,3). On the left of the diagrams (1) and (2) one finds the objects $G_{2,1}$ and F_3, respectively. These objects are presented diagrammatically in Figs. 1(c) and 1(b) of the present figure, respectively. On the right side of diagrams (1) and (2) one has the three-point objects that were designated as $\mathscr{A}$ and $\mathscr{D}$. These objects can be found in Fig. 1(d) and in (b) of the present figure.

function together with the integration over x_a contribute r^z. The Green's function of the bridge a-b in Fig. 1(c) contributes r/R^4, or r^1. The vertex A itself in diagrams 1 and 2 in Fig. 1(d) gives r^{-1}, and in total we find $r^{\zeta_2 + z}$ for these contributions. The same arguments give the same asymptotic behavior of diagram 3 shown in Fig. 1(d). This behavior should be compared with r^{ζ_2} for the homogeneous term, justifying the neglect of the inhomogeneous contribution. Note that small corrections to the exponents are not expected to erase the large gap $z \simeq 2/3$.

IV. TWO-POINT FUSION RULE FOR FOUR-POINT CORRELATION FUNCTIONS: THE EQUATION FOR THE EXPONENT μ

In this section we use the fact that we know exactly the ultraviolet exponent Δ to derive the fusion rule for four-point correlations. The n-point simultaneous correlation function of Eulerian velocity differences is defined as

$$F_n^{\alpha\beta\cdots\omega}(\mathbf{R}_1, \mathbf{R}_2, \ldots, \mathbf{R}_n) \equiv \langle \delta u_\alpha(\mathbf{r}_0 | \mathbf{R}_1, t)\, \delta u_\beta(\mathbf{r}_0 | \mathbf{R}_2, t) \cdots \delta u_\omega(\mathbf{r}_0 | \mathbf{R}_n, t) \rangle , \tag{4.1}$$

where $\delta\mathbf{u}$ was defined by (2.2) such that $\mathbf{R}_j=\mathbf{r}_j-\mathbf{r}_0$. By "fusion rules" we mean the scaling structure of F_n when two or more of the vector separations $\mathbf{R}_j$ tend to zero or to each other. In this section we discuss two-point fusion rules. Without loss of generality we can denote the coalescing coordinates as $\mathbf{r}_1$ and $\mathbf{r}_2$, and we will consider all distances of all the other coordinates $r_3,\ldots,r_n$ from $\mathbf{r}_0$ to be of the same order $O(R)\gg r_1,r_2$. To understand the fusion rules we will use diagrammatic language; at the end of the discussion one can recast the results into formal operator algebra without reference to diagrams [16]. The physical basis of this operator algebra (which allows multiscaling) and its appearance in turbulent systems with flux equilibria is an exciting subject that will be taken up fully in a separate publication [17].

A. Classification of the diagrams for the four-point correlator

In this section we will analyze the four-point correlator and the dissipation correlation function $K_{\epsilon\epsilon}$. The derivation begins with the examination of the four-point correlator $F_4^{\alpha\cdots\delta}(\mathbf{R}_1,\ldots,\mathbf{R}_4)$. This quantity is represented as an object with four wavy tails, each of which represents one of the velocity differences with coordinates $\mathbf{r}_1,\ldots,\mathbf{r}_4$. The trivial contributions to F_4, which we denote as $F_4^{(0)}$, are the three different products of F_2 which graphically are the "unlinked" (or "reducible") diagrams that stem from the Gaussian decomposition. The next set of diagrams that contributes to the four-point correlator is shown in Fig. 6. These are all the weakly linked diagrams in which the coordinates x_1,x_2 are linked to the coordinates x_3,x_4 via one propagator. As in the case of $\mathscr{G}_{n,m}$ we cannot have repeated one-propagator bridges since such contributions are resummed in the Dyson-Wyld line resummation. There are two possible types of bridges: (i) the bridge ends with a straight line and (ii) the bridge ends with a wavy line. In case (i) the diagrams can be resummed into diagram (1) of Fig. 6(a). In case (ii) the diagrams resum into diagram (2). The left part of diagram (1) is the Green's function $\mathscr{G}_{2,1}$. The diagrammatic presentation of this object is shown in Figs. 1(c) and 1(d). The right part of diagram (1) is the three-point object $\mathscr{A}$ shown in of Fig. 6(b) in terms of the dressed vertices A, B, and C, and the dressed propagators. The left part of diagram (2) in Fig. 6 is the third order correlation function F_3. Its diagrammatic representation in terms of dressed vertices and propagators is given by Fig. 7 of paper II, and in a more compact form in Fig. 6(c). We find again in this case the same three-point objects $\mathscr{A}$ and $\mathscr{D}$ that appeared already in panels (a) and (b) of Fig. 7 and in Fig. 1(d).

In addition to these weakly linked diagrams we have the strongly linked diagrams appearing in Fig. 7(b). All these are diagrams whose resummed parts are connected via a two-propagator bridge. The strongly linked diagrams are constructed as follows: locate the principal cross section of a diagram in the infinite expansion of F_4. Move from the principal cross section to the right and to the left until you find the first two-eddy reducible link, which is going to form the two-propagator bridge. The object between these two bridges is a contribution towards one of the resummed central objects on the RHS of the equation in Fig. 7, and see Fig. 8 for the beginning of the diagrammatic expansion for these objects. At this point collect all the diagrams with the same central object and resum them to the left and to the right. The result of this resummation is shown in Fig. 7. The four-point objects on the right and on the left of the central objects are exactly the same as those appearing in Fig. 5.

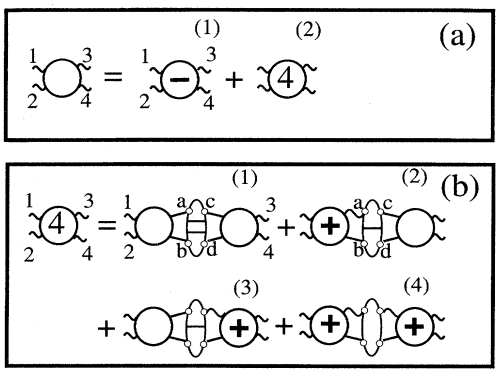

FIG. 7. (a) Diagrammatic representation of the irreducible four-point correlation function as a sum of weakly and strongly linked parts. Diagram (1) is the weakly linked part $F_4^{\rm wl}$ and diagram (2) is the strongly linked part $F_4^{\rm sl}$. $F_4^{\rm wl}$ is presented in Fig. 6. (b) Exact presentation of $F_4^{\rm sl}$. The elements appearing in this presentation are the four-point Green's functions $\mathscr{G}_{2,2}$ and $\mathscr{G}_{3,1}$ on the left side and on the right side of the diagrams, and three different new four-point objects. The notation used to distinguish the three new objects is with zero, one, or two horizontal lines inside. The diagrammatic representation of the new objects is shown in Fig. 8.

For an example of a fragment contribution to the right hand part of diagram (1) in Fig. 7(b), see Fig. 9.

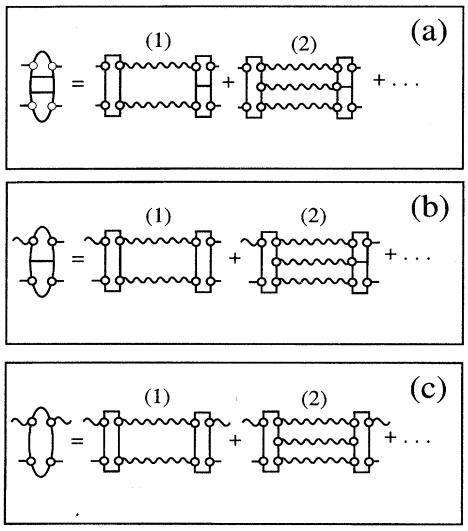

FIG. 8. Diagrammatic representation for the three different central blocks that appeared in Fig. 7. These are infinite order expansions in terms of contributions with increasing numbers of correlators in their principal cross section (i.e., 2, 3, 4, and more). The four-point objects in diagram (1) in each panel are the mass operators $\Sigma_{2,2}$ and $\Sigma_{3,1}$, which are the dressed rungs of the ladders whose presentation is shown in Figs. 3 and 4.

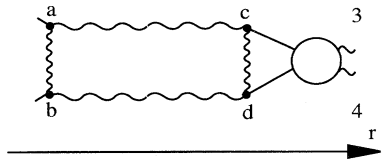

FIG. 9. An example of a fragment contribution to the right hand part of diagram (1) in Fig. 7.

B. Asymptotics

1. Strongly linked diagrams

Assume that $r_1, r_2 \sim r$ are much smaller than $r_3, r_4 \sim R$ but still in the inertial interval. Denote the structure whose outer coordinates are $\mathbf{r}_a, \mathbf{r}_b, \mathbf{r}_3, \mathbf{r}_4$ as $\Psi_m(\mathbf{r}_a, \mathbf{r}_b, \mathbf{r}_3, \mathbf{r}_4)$ with $m = 1, \ldots, 4$ according to the enumeration of the diagrams in Fig. 7. Diagrams (1)–(4) can now be written analytically as

$$(1) = \int dx_a dx_b \mathscr{G}_{2,2}(\mathbf{r}_0 | x_1, x_2, x_a, x_b) \Psi_1(\mathbf{r}_a, \mathbf{r}_b, \mathbf{r}_3, \mathbf{r}_4), \tag{4.2}$$

$$(2) = \int dx_a dx_b \mathscr{G}_{3,1}(\mathbf{r}_0 | x_1, x_2, x_a, x_b) \Psi_2(\mathbf{r}_a, \mathbf{r}_b, \mathbf{r}_3, \mathbf{r}_4), \tag{4.3}$$

$$(3) = \int dx_a dx_b \mathscr{G}_{2,2}(\mathbf{r}_0 | x_1, x_2, x_a, x_b) \Psi_3(\mathbf{r}_a, \mathbf{r}_b, \mathbf{r}_3, \mathbf{r}_4), \tag{4.4}$$

$$(4) = \int dx_a dx_b \mathscr{G}_{3,1}(\mathbf{r}_0 | x_1, x_2, x_a, x_b) \Psi_4(\mathbf{r}_a, \mathbf{r}_b, \mathbf{r}_3, \mathbf{r}_4). \tag{4.5}$$

Suppose that we can argue that all the functions $\Psi_m(\mathbf{r}_a, \mathbf{r}_b, \mathbf{r}_3, \mathbf{r}_4)$ contribute at r_a, r_b smaller contributions than those of $\Phi(\mathbf{r}_a, \mathbf{r}_b)$ in Eq. (3.15). If so, we can think of these Ψ functions as generalized perturbations δD that leave the r_{12} dependence universal. According to (3.12) and (3.13) the main r_{12} dependence comes from diagrams (1) and (3) and it is $r_{12}^{\zeta_2}$.

To demonstrate that this is indeed the case we can look at a typical diagrammatic contribution to any of the diagrams in Fig. 7. For example, the first contribution to $\Psi_1(\mathbf{r}_a, \mathbf{r}_b, \mathbf{r}_3, \mathbf{r}_4)$ is shown in Fig. 8. This particular example comes from diagram (1) in Fig. 8(b) upon taking diagram (1) for the rung in Fig. 2. Take $r_a \sim r_b$ and examine the dependence on r_a. The two vertices contribute r_a^{-2}. The correlator in between is worth $r_a^{\zeta_2}$. The two stretched correlators connecting to larger coordinates contribute $r_a^{2\zeta_2}$. The two time integrals in the vertices c and d contribute r_a^{2z} where z is the dynamic scaling exponent, $\tau(r) \propto r^z$ (and see details in paper I). In total we have r_a^{β} with $\beta = 3\zeta_2 + 2z - 2$. This has to be compared with the exponent α of $\Phi(\mathbf{r}_a, \mathbf{r}_b)$, which is $\alpha = \zeta_4 - 2$ according to (3.16). In K41 evaluation $\beta = 4/3$ whereas $\alpha = -2/3$. The gap is so large that small corrections to K41 cannot change the fact that the exponent of Φ is dominant, as we want. Note that this demonstration is perturbative (order by order with only the lowest order done explicitly), but again the magnitude of the gap is sufficient to validate the claim.

Exactly the same arguments hold for the contribution (4.4). The contributions (4.3) and (4.5) relate to the asymptotic behavior of the other Green's function $\mathscr{G}_{3,1}$. It is clear, however, that due to the result in (3.20) the exponents are the same.

2. Weakly linked diagrams

The analysis of the weakly linked diagrams in this case follows closely the discussion of Sec. III C. The diagrams can be resummed as shown in Fig. 6(b). We have two contributions; in diagram (a) we have on the left F_3 and on the right the object defined in the second line of the figure. In diagram (2) we have $\mathscr{G}_{2,1}$ (shown in Fig. 7) on the left and the object defined in the third line of Fig. 6(b). In the limit $r_1, r_2 \sim r \ll r_3, r_4 \sim R$ the integrals over r_b in both diagrams contribute mainly in the region $r_b \sim R$. Accordingly in diagram (2) we have the same situation that was discussed in Sec. III C, and see Fig. 4(b). Diagram (1), on the other hand, may be bounded from above by the asymptotics of F_3 with one large and two small coordinates. Under the property of rigidity one can see that this correlator is independent of the large coordinate, and is therefore proportional to r^1. Again we have a gap, and this gap can only increase if we take into account the time integral of the x_b vertex. Thus the weakly linked diagrams can be again disregarded.

C. Two-point correlation of the energy dissipation

At this point we can employ our results to evaluate the correlation function (1.4). We first write this quantity in a way that makes its relation to F_4 clear:

$$\begin{aligned} K_{\epsilon\epsilon}(R) = \nu^2 \lim_{r_{12}, r_{34} \to 0} \lim_{r_{13} \to R} & \nabla_{1\alpha} \nabla_{2\beta} \nabla_{3\gamma} \nabla_{4\delta} \\ & \times [F_4^{\alpha'\beta'\gamma'\delta'}(\mathbf{r}_1, \mathbf{r}_2, \mathbf{r}_3, \mathbf{r}_4) \\ & - F^{\alpha'\beta'}(\mathbf{r}_1, \mathbf{r}_2) F^{\gamma'\delta'}(\mathbf{r}_3, \mathbf{r}_4)] [\delta_{\alpha\beta}\delta_{\alpha'\beta'} \\ & + \delta_{\alpha\beta'}\delta_{\alpha'\beta}][\delta_{\gamma\delta}\delta_{\gamma'\delta'} + \delta_{\gamma\delta'}\delta_{\gamma'\delta}]. \end{aligned} \tag{4.6}$$

This is a generalization of the situation discussed above in the sense that we have two pairs of coalescing points, r_1, r_2 and r_3, r_4. By examining Fig. 8(a) we can see that the symmetry allows us to treat each coalescing pair separately. In the limit r_{12} and r_{34} being much smaller than R each pair of derivatives $\nabla_1 \nabla_2$ and $\nabla_3 \nabla_4$ will contribute a divergent term proportional to $r_{12}^{-\Delta}$ and $r_{34}^{-\Delta}$, respectively. The dependence on R can be found knowing that the overall exponent of F_4 is ζ_4. Thus the overall scaling exponent of the quantity in the RHS (4.6) must be $\zeta_4 - 4$. Using the fact that $\Delta = 2 - \zeta_2$ we conclude that

$$\nabla_1 \nabla_2 \nabla_3 \nabla_4 F_4(\mathbf{r}_1, \mathbf{r}_2, \mathbf{r}_3, \mathbf{r}_4) \sim \bar{\epsilon}^{4/3} [r_{12} r_{34}]^{-\Delta} R^{\zeta_4 - 2\zeta_2} \ell^{4/3 - \zeta_4}, \tag{4.7}$$

where for simplicity we suppressed the vector indices and we made the relation dimensionally correct by introducing some renormalization scale ℓ. Note that for K41 scaling exponents the factor $\bar{\epsilon}^{4/3}$ fixes the correct dimensionality of the

RHS. For anomalous exponents one needs a renormalization scale to take care of the difference between the K41 and the actual value of the exponent ζ_4. It will be shown later that this renormalization scale must be the outer scale L. At this point it does not matter. The divergence in the limit indicated in (4.6) should be understood in light of the full theory for F_4, in which the ν diffusive terms are explicit. The role of these terms is precisely to truncate the divergence that is implied by (4.6). As a consequence the divergence is only applicable in the inertial range with r_{12}, r_{34} larger than some dissipative scale, whereas in the dissipative regime the divergence disappears. The value of this dissipative scale is *a priori* unknown. We are going to denote it as $\eta^{(4)}_{2,2}(R)$, recalling that it is the dissipative scale of a four-point correlation when two pairs of points coalesce, and for all that we know it may be a function of the remaining inertial scale R. Thus for evaluating $K_{\epsilon\epsilon}(R)$ via inertial range values we must replace the limit $r_{12}, r_{34} \to 0$ by $r_{12} = r_{34} = \eta^{(4)}_{2,2}(R)$. Thus we can write

$$K_{\epsilon\epsilon} \sim \nu^2 \bar{\epsilon}^{4/3} [\eta^{(4)}_{2,2}(R)]^{-2\Delta} R^{\zeta_4 - 2\zeta_2} \ell^{4/3 - \zeta_4}. \tag{4.8}$$

It is important to realize that in general the dissipative scale that appears here differs from the Kolmogorov scale that is introduced usually. The latter is defined from the definition of $\bar{\epsilon}$, which is

$$\bar{\epsilon} \sim \nu \lim_{r_{12} \to \eta} \nabla_1 \nabla_2 S_2(r_{12}). \tag{4.9}$$

In the same spirit we can write the structure function $S_2(R)$ as

$$S_2(R) \sim \bar{\epsilon}^{2/3} R^{\zeta_2} \ell^{2/3 - \zeta_2}, \tag{4.10}$$

where again the renormalization scale ℓ fixes the dimensions. From the last two equations one can compute

$$\bar{\epsilon}^{1/3} \sim \nu \eta^{-\Delta} \ell^{2/3 - \zeta_2}. \tag{4.11}$$

Substituting this in (4.8) we get finally

$$K_{\epsilon\epsilon}(R) \sim \bar{\epsilon}^2 \left(\frac{\ell}{R} \right)^{2\zeta_2 - \zeta_4} \left(\frac{\eta}{\eta^{(4)}_{2,2}(R)} \right)^{2\Delta}. \tag{4.12}$$

The final scaling law depends on the R dependence of $\eta^{(4)}_{2,2}(R)$, which is not known at the present time. The first scenario is obtained if one assumes that there exists only one dissipative scale η, which is determined by Eq. (4.11). In this case $\eta^{(4)}_{2,2}(R)$ is R independent and equals η. It will turn out that the renormalization scale ℓ is the outer scale of turbulence L. From this we get the "bridge" relation

$$\mu = 2\zeta_2 - \zeta_4 \quad \text{(first scenario)}. \tag{4.13}$$

This "bridge" relation is exact in the case of the Kraichnan model of passive scalar convection as shown in [19]. In general we need to consider a second scenario in which $\eta^{(4)}_{2,2}(R)$ does depend on R. Assuming that it scales with R like

$$\eta^{(4)}_{2,2}(R) \propto R^x, \tag{4.14}$$

we get

$$\mu = 2\zeta_2 - \zeta_4 - 2x(2 - \zeta_2) \quad \text{(second scenario)}, \tag{4.15}$$

where (3.19) has been used. We will return to the numerical estimate of the exponent x and the bridge in Sec. VII.

V. TWO-POINT FUSION RULE FOR MANY-POINT CORRELATION FUNCTIONS: THE DERIVATION OF J_n

In this section we evaluate the scaling exponent of the dissipative terms J_n (2.40) of the balance equations. The strategy is to expose the divergence with the ultraviolet cutoff η for which we have an exact evaluation of the exponent Δ. Together with the overall scaling, which is determined by ζ_n we will be able to discuss the R dependence of $J_n(R)$ within our two main scenarios. Afterwards we will evaluate the interaction term $D_n(R)$ and use the balance equation as a nonperturbative constraint to deduce the scaling exponents ζ_n.

A. Classification of the diagrams as weakly linked or strongly linked

The n-point correlation function F_n can be represented symbolically as an object with n wavy tails, each one representing one of the n coordinates $\mathbf{r}_j$ associated with a velocity difference $\delta u(\mathbf{r}_0 | \mathbf{R}_j)$. We remind the reader that for simultaneous correlation functions one can use either the Eulerian differences (2.2) or the BL velocity differences (2.11), since they are the same at $t = 0$. In the diagrammatic expansion for the simultaneous F_n there appear time dependent correlations, and there the theory calls for the use of BL velocity differences.

Having two special coordinates $\mathbf{r}_a$ and $\mathbf{r}_b$ we can ask how the part of the diagram containing these coordinates is linked to the rest of the diagram. This part can be connected via one propagator, see Fig. 10(a), via two propagators, see Fig. 10(b), or via three or more. As in the case of the four-point correlator and four-point Green's function a one-propagator bridge cannot appear again between the legs carrying the designation a, b and the body of the diagram. In total one has $n(n-1)/2$ weakly linked contributions in each of which the role of the weakly linked pair is played by one of the available pairs of legs. In addition one has also double weakly linked contributions with two bridges made of a single propagator that connects different pairs, etc., and see diagram (3) in Fig. 10(a). Such diagrams do not play an important role in our analysis. In displaying the diagrams in Fig. 10(a) we have included the bridge (which is a correlator or a Green's function) in the object on the left of the bridge. For this reason the object on the right of the bridge begins with a vertex x_c. According to our convention this vertex is denoted by a small empty circle. The diagrams appearing in Fig. 10(a) should already look familiar. In diagram (1) we again have an F_3 correlator on the left, integrated over x_c with an $(n-1)$-point object on the right. This is the generalization of diagram (2) in Fig. 6(a). In diagram (2) we have the three-point Green's function $\mathcal{G}_{2,1}$ of Eq. (3.1) on the left, again integrated over x_c with a different $(n-1)$-point object. This can be compared with diagram (1) in Fig. 6(a). For our

considerations the precise nature of the object on the right is irrelevant.

Similarly, all the contributions with two propagators serving as links can be resummed into the objects shown in Fig. 10(b). Again we included the two propagators that form the bridges in the objects appearing to the left of the bridges. Again this results in the n-point objects on the right being attached to the left by two vertices x_a and x_b. Their interpretation is as follows: diagram (1) is a fourth order correlator linked via integrals over x_a and x_b to the rest of the diagram. In diagram (2) the linked object is $\mathscr{G}_{3,1}$ (3.4). In diagram (3) the linked object is precisely our familiar second order Green's function $\mathscr{G}_{2,2}$.

Links with three or more propagators have been already taken into account in this presentation. This classification of the diagrams is based on starting with the two special coordinates x_1, x_2 on the left, and then moving to the right and stopping when the first one-propagator bridge appears. All these diagrams are resummed exactly into one of the contributions in Fig. 10(a). If there is no one-propagator bridge, we start again from the left and monitor all the two-propagator bridges, ending with the last pair. All such diagrams are resummed into one of the contributions in Fig. 10(b).

B. Asymptotic tensor structure and fusion rules

In this section we find the tensor structure of $F_n^{\alpha\beta\cdots\omega}$ when the two coordinates r_1, r_2 are much smaller than the rest. When all the coordinates $r_3, \ldots, r_n$ are of the order of $R \gg r$, whereas r_1, r_2 are small, the property of rigidity that was demonstrated in paper II requires that the main contribution to the integrations over r_a and r_b in the diagrams of Fig. 10(b) come from the region $r_a \sim r_b \sim R$. In this case we have a very similar situation to the one discussed before in the context of Fig. 7(b). Accordingly the three objects on the left of the double bridge of the diagrams in Fig. 10(b) are familiar and have the same scaling with respect to r, i.e., r^{ζ_2}. The weakly linked contributions shown in Fig. 10(a) have the same objects on the left of the bridge as those shown in Fig. 6(a) for F_4, and they are irrelevant for the same reasons.

Limiting our attention to strongly linked diagrams with two-propagator links we examine now the tensor structure of $F_n^{\alpha\beta\cdots\omega}$. We need to keep in mind Eq. (3.13), which means that when $r_1, r_2 \to 0$ $\delta F^{\alpha\beta} \propto F^{\alpha\beta}$. In light of Fig. 5 the objects $\mathscr{G}_{2,2}^{\alpha\beta\gamma\delta}$ and $\mathscr{G}_{3,1}^{\alpha\beta\gamma\delta}$ have the same asymptotics. We have found before that they are proportional to $F^{\alpha\beta}(\mathbf{r}_1, \mathbf{r}_2)$. Diagram (1) is again proportional to the same quantity in light of Fig. 7(b). We can therefore write the following fusion rule:

$$\lim_{r_1, r_2 \to 0} F_n^{\alpha\beta\gamma\cdots\omega}(\mathbf{r}_1, \mathbf{r}_2, \mathbf{R}_3, \ldots, \mathbf{R}_n) = F^{\alpha\beta}(\mathbf{r}_1, \mathbf{r}_2)\Psi_{n-2}^{\gamma\cdots\omega}(\mathbf{R}_3, \ldots, \mathbf{R}_n). \tag{5.1}$$

Here Ψ_{n-2} is a homogeneous function of its arguments when they are all in the inertial range. The scaling exponent of Ψ_{n-2} is $\zeta_n - \zeta_2$. The reason for that is clear: the scaling exponent of F_n is ζ_n, but one ζ_2 is already carried by $F^{\alpha\beta}$. The tensor structure of $\Psi_{n-2}^{\gamma\cdots\omega}$ is not known in detail at this point, except that it conforms with incompressibility and isotropy. In other words, this quantity is independent of the vectors $\mathbf{r}_1, \mathbf{r}_2$.

C. The evaluation of $J_n(R)$

At this point we are ready to evaluate the dissipative terms in the balance equation. The equation to consider is (2.40). As was done in the context of the evaluation of $K_{\epsilon\epsilon}$ we evaluate the quantity in the inertial interval, and then replace the limits $d_\beta \to 0$ with the ultraviolet cutoff $d_\beta = \eta$. In the inertial interval we write

$$T_{2m}^{\alpha\alpha}(d_\beta \mathbf{e}_\beta, d_\beta \mathbf{e}_\beta, \mathbf{R}) = F^{\alpha\alpha}(d_\beta \mathbf{e}_\beta, d_\beta \mathbf{e}_\beta)\Psi_{2m-2}^{(1)}(R), \tag{5.2}$$

$$T_{2m}^{\alpha\gamma\alpha\gamma}(d_\beta \mathbf{e}_\beta, d_\beta \mathbf{e}_\beta, \mathbf{R}) = F^{\alpha\gamma}(d_\beta \mathbf{e}_\beta, d_\beta \mathbf{e}_\beta)\Psi_{2m-2}^{(2)\alpha\gamma}(\mathbf{R}), \tag{5.3}$$

where the fusion rule (5.1) has been used. The two functions Ψ satisfy

$$\Psi_{2m-2}^{(1)}(R) = A_1 R^{\zeta_{2m} - \zeta_2}, \tag{5.4}$$

$$\Psi_{2m-2}^{(2)\alpha\gamma}(\mathbf{R}) = A_2 R^{\zeta_{2m} - \zeta_2}\left[\delta_{\alpha\gamma} - a_m \frac{R_\alpha R_\gamma}{R^2}\right], \tag{5.5}$$

with A_1 and A_2 being constants. The reason for these forms stems again from the fusion rule. $\Psi^{(1)}$ and $\Psi^{(2)\alpha\beta}$ are scalar and two-tensor, respectively, and we wrote their general forms for isotropic conditions. Incompressibility dictates the value of a_m but we do not need to compute it for our purposes. Lastly we note that

$$F^{\alpha\gamma}(d_\beta \mathbf{e}_\beta, d_\beta \mathbf{e}_\beta) = S_2^{\alpha\gamma}(d_\beta) \propto d_\beta^{\zeta_2}\left[\delta_{\alpha\gamma} - a_1 \frac{R_\alpha R_\gamma}{R^2}\right]. \tag{5.6}$$

Incompressibility requires the relation $a_1 = \zeta_2/(1+\zeta_2)$.

Presently we can substitute all this knowledge into Eq. (2.40). One should note that in the inertial range the velocity field is not smooth ($\zeta_2 < 2$), and we may run into the danger that the quantity computed depends on the angle between the vectors $\mathbf{d}, \mathbf{R}$. However, the procedure implied requires taking the limit such that all d_β are the same and equal the characteristic dissipative scale of J_{2m}. We will denote the dissipative scale of J_{2m} as $\eta_2^{(2m)}(R)$ such that the upper index denotes the total number of points and the lower index the number of coalescing points. The fact that this is the appropriate limit can be checked explicitly by introducing the tensor structure to all the quantities appearing in the limit. The condition that all the components d_β are the same guarantees that the limit is independent of the angle. The result of the substitution is

$$J_{2m}(R) = 2mC_{2m}\nu[\eta_2^{(2m)}(R)]^{-\Delta} R^{\zeta_{2m} - \zeta_2} \ell^{2m/3 - \zeta_{2m}}. \tag{5.7}$$

We again use a renormalization scale ℓ to fix the dimensions. It will turn out that this renormalization scale is the outer scale of turbulence L.

We see that again we have an unknown R dependence of a viscous cutoff scale. We will proceed by examining again two scenarios; the first one assumes that there exists only one

viscous scale, which is R independent, and the second allows a characteristic exponent y_{2m}:

$$\eta_2^{(2m)}(R) \propto R^{y_{2m}}. \tag{5.8}$$

We discuss the two scenarios separately.

1. First scenario

Even in the first scenario we will see that the form (5.7) of J_n is sufficient for the calculation of the exponents ζ_n through the use of the balance equation only if the dependence of ζ_n on n is linear (i.e., in the β model). If the dependence is nonlinear (multiscaling) we need to determine the coefficients C_{2m} exactly. To do so we now rewrite Eq. (5.7) in terms of the structure functions S_n. This way of writing is compelling only when the scaling exponents are a nonlinear function of n, as will be clear in a moment. We write S_n in the form

$$S_{2m}(R) \sim \bar{\epsilon}^{3m/3} R^{\zeta_{2m}} \ell^{2m/3-\zeta_{2m}}. \tag{5.9}$$

This form is the generalization of (4.10) and is the most general form that conforms with scaling and is dimensionally correct. Using Eqs. (4.10) and (4.11) in (5.9) we find the convenient representation

$$J_{2m}(R) = m \frac{C_{2m}}{C_2} J_2 \frac{S_{2m}(R)}{S_2(R)} \quad \text{(first scenario)}. \tag{5.10}$$

We stress that this result is valid only when $R \gg \eta$, since we used the asymptotics, and only when ζ_n is nonlinear in n. If the scaling exponents are linear in n we can have other contributions like S_{2m+1}/S_3 or any other ratio whose scaling exponent is $\zeta_{2m}-\zeta_2$. In particular (5.10) is not applicable to Burgers turbulence.

Next we will employ an idea that is due to Kraichnan [18] to argue that in the multiscaling case the coefficient C_{2m} is m independent. Begin with Eq. (2.22), which is rewritten as an integral over the distribution function $P(\mathbf{w})$:

$$J_{2m}(R) = \int d\mathbf{w} P(\mathbf{w}) w^{2(m-1)} w_\alpha \langle [\nabla_r^2 + \nabla_{r_0}^2] w_\alpha | \mathbf{w} \rangle. \tag{5.11}$$

Here $\langle [\nabla_r^2 + \nabla_{r_0}^2] w_\alpha | \mathbf{w} \rangle$ is the conditional average of $[\nabla_r^2 + \nabla_{r_0}^2] w_\alpha$ conditioned on a given value of $\mathbf{w}(\mathbf{r}_0|\mathbf{r}_0+\mathbf{R},t)$. The point to observe now is that the only way to recover our result (5.10) when ζ_n is a nonlinear function of n is to demand that the conditional average satisfies

$$\langle [\nabla_r^2 + \nabla_{r_0}^2] w_\alpha | \mathbf{w} \rangle = C \frac{w_\alpha(\mathbf{r}_0|\mathbf{r}_0+\mathbf{R},t)}{S_2(R)}, \tag{5.12}$$

where C is some coefficient that is evidently independent of m. It follows that C_{2m} is independent of m.

Note that this result for the conditional average is only valid in the inertial range of scales, since it has been derived using Eq. (5.10), which is only valid there. Notwithstanding we can employ (5.12) right away to compute the vector quantity $J_{2m+1}^\alpha(R)$. Writing (2.27) again as an integral over the distribution function $P(\mathbf{w})$ and substituting (5.12) we find

$$J_{2m+1}^\alpha(R) = \frac{(2m+1)}{2} J_2 \frac{S_{2m+1}^\alpha(R)}{S_2(R)}. \tag{5.13}$$

We can thus summarize this section with a result that is valid for both odd and even n by using the scalar counterpart of the vector quantities:

$$J_n(R) = J_2 \frac{n S_n(R)}{2 S_2(R)} \quad \text{(first scenario)}. \tag{5.14}$$

This is the final result of this subsection. We note that such a scaling formula for J_{2m} was suggested by Kraichnan in the context of passive scalar advection [18], and was derived in [19].

2. Second scenario

In this scenario we take into account the possible R dependence of $\eta_2^{(2m)}(R)$ according to (5.8). This will change Eq. (5.10) into

$$J_{2m}(R) = m \frac{C_{2m}}{C_2} J_2 \frac{S_{2m}(R)}{S_2(R)} \left[\frac{\eta}{\eta_2^{(2m)}(R)} \right]^\Delta \quad \text{(second scenario)}. \tag{5.15}$$

We will explore this scenario by incorporating at this point the Kolmogorov refined similarity hypothesis. We caution the reader that this step does not follow from our theoretical development, and is used here to determine the set of exponents y_{2m}, which at present are not available from first principles.

The essence of the refined similarity hypothesis [21] is that the average of the energy dissipation rate $\epsilon(\mathbf{r}_0,t)$ conditional on a given velocity difference $\delta\mathbf{u}(\mathbf{r}_0|\mathbf{R},t)$ is proportional to third power of the latter:

$$\langle \epsilon(\mathbf{r}_0,t) | \delta\mathbf{u}(\mathbf{r}_0|\mathbf{R},t) \rangle \sim [\delta u(\mathbf{r}_0|\mathbf{R},t)]^3/R. \tag{5.16}$$

This relation means that

$$J_n \sim S_{n+1}(R)/R. \tag{5.17}$$

Comparing with Eq. (5.15) we find the exponents

$$y_n = \frac{\zeta_n - \zeta_{n-1} + \zeta_3 - \zeta_2}{2-\zeta_2}. \tag{5.18}$$

Note that this is a prediction for the dissipative scale of a correlation function of the type $\langle [\delta u(\mathbf{r}_0|\mathbf{r},t)]^2 [\delta u(\mathbf{r}_0|\mathbf{R},t)]^{n-2} \rangle$ when $r \ll R$. The fusion rules derived above mean that the scaling form of this function is $r^{\zeta_2} R^{\zeta_n - \zeta_2}$ for $r > \eta_2^{(n)}$. The present result states which is the smallest R-dependent r for which this scaling form is tenable. Repeating the steps involving the distribution function $P(\mathbf{w})$ we conclude with the form of J_n alternative to (5.14) which holds in the second scenario:

$$J_n(R)=J_2\frac{nS_{n+1}(R)}{2S_3(R)} \quad \text{(second scenario)}. \tag{5.19}$$

D. The dynamical exponent z_n

As a windfall profit from the calculation of J_n we can address now the dynamical exponents associated with the n-point correlations. We will see that in the first scenario they are all the same, whereas in the second scenario there is an n dependence. The dynamical exponent z_n is defined by the assumption of scale invariance of the n-point, n-time correlation function of the BL velocity differences in the form

$$F_n(\lambda\mathbf{R}_1,\lambda^{z_n}t_1,\ldots,\lambda\mathbf{R}_n,\lambda^{z_n}t_n)=\lambda^{\zeta_n}F_n(\mathbf{R}_1,t_1,\ldots,\mathbf{R}_n,t_n). \tag{5.20}$$

The meaning of this form is that the typical time scale associated with n-point quantities scales like R^{z_n} when R is changed.

1. First scenario

In this scenario we can examine Eq. (2.20) and realize that J_n, which according to (5.14) is $nJ_2S_n(R)/S_2(R)$, gives us the desired time scale. In fact, the R dependence of the time scale is determined entirely by $S_2(R)$, and therefore

$$z_n=\zeta_2 \quad \text{for all } n. \tag{5.21}$$

This is a prediction that to our knowledge has never been tested either in experiments or simulations. It is interesting to notice that independently of the question of multiscaling in the spatial scale, the temporal scaling is simple.

It is amusing to try to understand (5.21) intuitively. In doing so we want to separately understand why $z_2=\zeta_2$ and then why all z_n are the same. The first finding seems to contradict the naive dimensional evaluation of $\tau_2(R)$ as $R/\sqrt{S_2(R)}$, which is the "turn-over" time of R eddies with characteristic velocity $\sqrt{S_2(R)}$. This evaluation would lead to $z_2=1-\zeta_2/2$, which is not consistent with (5.21).

Another way of thinking that leads to the right result is to estimate the rate of energy dissipation as the ratio of energy of R motions, which is $S_2(R)$, by the time scale $\tau_2(R)$. Since the rate of energy dissipation is R independent (being $\bar{\epsilon}$), this fixes $\tau_2(R)$ to scale as R^{ζ_2}.

The n independence of z_n is more subtle, and is not recaptured in the second scenario. Here we just want to point out that this result entails a prediction about the measurement of dimensionless ratios of structure functions, like $S_3/S_2^{2/3}$, S_4/S_2^2, etc. in decaying turbulence. The prediction is that such relations are R dependent but not time dependent. We believe that this is not in contradiction with what is known about decaying turbulence behind a grid.

2. Second scenario

In the second scenario we use (5.19) and repeat the steps leading to the evaluation of the dynamical exponents z_n. Instead of $z_n=\zeta_2$ we find now the following n dependence:

$$z_n=\zeta_n+\zeta_3-\zeta_{n+1}. \tag{5.22}$$

In the case of linear dependence of ζ_n on n this result is identical to the previous one. However, in a multiscaling situation the n dependence is nontrivial. Hölder inequalities imply that in this case z_n is larger than ζ_2. This is also a testable result.

VI. THE INTERACTION TERM IN THE BALANCE EQUATION

In this section we present the analysis of the interaction term D_n; see (2.36) and (2.37). The question that was left at the end of Sec. II C 1 is whether the integral over $\mathbf{r}_1$ converges. Order-by-order analysis of the type presented in paper I indicates that the answer is yes. However, we need now to consider the nonperturbative answer using what we have learned so far.

A. Locality of the integral in the interaction term

In order to do this we need further asymptotic properties of the functions T_n, which appear in the integral. For brevity we will suppress the tensor indices of these objects, and consider even and odd n in the same way. The convergence of the integrals depends on $T_n(\mathbf{R}+\mathbf{r}_1,\mathbf{R}+\mathbf{r}_1,\mathbf{R})$ and $T_n(\mathbf{r}_1,\mathbf{r}_1,\mathbf{R})$ when $r_1\gg R$ and when $r_1\ll R$. So far we have only analyzed $T_n(\mathbf{r}_1,\mathbf{r}_1,\mathbf{R})$ when $r_1\ll R$. The full analysis of the two unknown asymptotics is as involved as the one presented above, and we will present them in a separate publication [17]. Here we will simply employ the results that we need for the present analysis.

Consider first $T_n(\mathbf{R}+\mathbf{r}_1,\mathbf{R}+\mathbf{r}_1,\mathbf{R})$ for r_1 small. The analysis in [17] shows that for $r_1\ll R$,

$$T_n(\mathbf{R}+\mathbf{r}_1,\mathbf{R}+\mathbf{r}_1,\mathbf{R})-S_n(R)\propto S_2(r_1)\propto r_1^{\zeta_2}. \tag{6.1}$$

Next consider $T_n(\mathbf{r}_1,\mathbf{r}_1,\mathbf{R})$ in the limit $r_1\gg R$. The analysis in [17] leads to

$$T_n(\mathbf{r}_1,\mathbf{r}_1,\mathbf{R})\propto R^{\zeta_{n-2}}r_1^{\zeta_n-\zeta_{n-2}}. \tag{6.2}$$

These results can be employed now in the integral for D_{2m}. In this integral we have the projection operator $\overleftrightarrow{\mathbf{P}}$, which has a δ function and a longitudinal part. It was demonstrated in Sec. II that the δ function leads to the expression (2.34), as if there were no pressure. The longitudinal part of $\overleftrightarrow{\mathbf{P}}(\mathbf{r}_1)$ is proportional to $1/r_1^3$. The integral $\int d\mathbf{r}_1\overleftrightarrow{\mathbf{P}}(\mathbf{r}_1)$ by itself diverges logarithmically. The rest of the integrand (i.e., $\partial T_n/\partial r_{1\gamma}$) behaves like $r_1^{-\Delta}r_{1\gamma}$. Simple power counting indicates that the integral diverges on the whole in the ultraviolet region. In fact, this power counting is misleading, since the integration over the angles vanishes. The projection operator is an even function under the inversion of $\mathbf{r}_1$, whereas the leading term of the rest of the integrand is odd. The next term in the expansion of $\partial T_n/\partial r_{1\gamma}$ is even under the inversion of $\mathbf{r}_1$, and is of the order of $r_1^{\zeta_2}$. The resulting integral $\int dr_1 r_1^{\zeta_2-1}$ converges in the ultraviolet.

Note that this analysis indicates that each of the two terms in the integral for D_n converge in the ultraviolet independently. In fact, we see from Eqs. (6.1) and (5.2) that the two terms have precisely the same asymptotics, and they may exactly cancel in the limit. In addition we see from (2.36)

that the leading asymptotics of the two terms cancels exactly also in the infrared. These facts are important; we will argue below that the leading scaling behavior for D_n, which is naively calculated from each term separately, may cancel, and the actual scaling is determined by the next order contribution. This will be a mechanism for multiscaling.

Notwithstanding the exact cancellation of the leading infrared behavior we need to examine the infrared convergence of the integral. Each one of the terms in the integrand of D_{2m} has the asymptotic form $\int (dr_1/r_1)\partial r_1^{\zeta_n-\zeta_{n-2}}/\partial r_1$, which converges separately in the infrared. The difference should converge even faster.

In summary, we argued here that the proof of locality of the integral for D_{2m} extends beyond order-by-order considerations. Similar arguments allow reaching the same conclusion for the integrals in D_{2m+1}.

One should stress here that the above constitutes actually a nonperturbative derivation of the cascade picture of turbulence. The fact that the interaction term is local in R means that the transfer of energy down the scales is not achieved in a long ranged jump directly from the outer to the viscous scales, as these do not appear in the integrals comprising D_n. What we have is a stepwise process that cascades down from the largest to the smallest scales.

B. Evaluation of D_n

We recall that when the effect of pressure is unimportant, the evaluation of D_n is

$$D_n(R)=\frac{dS_{n+1}(R)}{dR}. \tag{6.3}$$

The conclusion of the last subsection is that the main contribution to the integrals appearing in D_n comes from the region $r_1 \sim R$. As a result we can argue that this evaluation is also applicable up to n-dependent dimensionless constants also when pressure is acting. To see this we go back to Eq. (2.36) and focus on the second contribution. For $\mathbf{r}_1=\mathbf{R}$ the T tensor is exactly $S_{n+1}(R)$. The r_1 derivative is acting on two out of $2m+1$ of the coordinates. Thus for $\mathbf{r}_1=\mathbf{R}$ the derivative is exactly $2/(2m+1)$ times an R derivative on S_{2m+1}. The first term has the same property at $r_1=0$. It is thus plausible that the evaluation (6.3) remains valid, and the coefficient is proportional to $4m/(2m+1)$. Writing the evaluation as

$$D_n(R)=b_n\frac{dS_{n+1}(R)}{dR}, \tag{6.4}$$

we expect that b_n becomes n independent for large n. One can check that this expectation is supported by the asymptotic analysis of the T tensors in the sense that for large and small r_1 the asymptotic behavior of the integrand becomes n independent for large n. Since for r_1 of the order of R the coefficient is unity, we conclude that it is very likely that b_n becomes n independent.

On other hand it is not impossible that b_n is zero altogether. In other words the interaction term as shown in Eqs. (2.36) and (2.37) may have a cancellation of the leading scaling behavior, which is valid for every one of the terms in the integrals separately. We will therefore also study now the next order term that will be the proper evaluation of D_n *if* the leading evaluation indeed cancels. These two evaluations will be tied naturally with the first and second scenarios for the valuation of J_n.

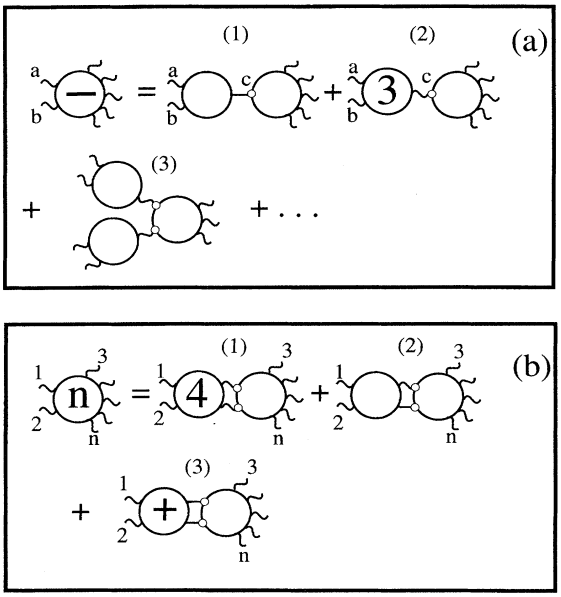

FIG. 10. Diagrammatic representation of n-point correlation functions. (a) Weakly linked contributions. Diagrams (1) and (2) are the generalization of diagrams (1) and (2) for F_4 shown in Fig. 6(a). Diagram (3) is an example of a weakly linked contribution with two one-propagator bridges. Such contributions do not appear in the case of F_4. (b) Strongly linked contributions to F_n, considering the legs designated as 1 and 2 special. In diagram (1) one has F_4 on the left; in diagrams (2) and (3) one has $G_{3,1}$ and $G_{2,2}$, the same objects that appeared in of Fig. 7(b) for F_4.

To evaluate the next order scaling contribution of D_n we need to return to the diagrammatic expansion of F_n, Fig. 10. In the discussion in Sec. V we explained that in the asymptotic regime of two small coordinates the weakly linked diagrams are negligible compared with the two-propagator bridged contributions, even in K41 scaling. Now, however, we are interested in these diagrams when all the coordinates are of the same order, and it is evident that, with respect to K41, they all have the same scaling with R. In fact, the unlinked contributions to F_n, which are obtained from the Gaussian decomposition (i.e., all the contributions F_pF_q with $p+q=n$), also have the same K41 evaluation. In addition we have a set of weakly linked contributions such as the ones displayed in Fig. 10(a). Again they have the same scaling in K41. Accordingly we need to think which contributions are dominant when the leading scaling $(R/L)^{\zeta_n}$ cancels in the evaluation of D_n. (Since we are going to show that anomalous scaling requires the normalization scale to be L, we assume this in the present discussion without further ado.)

The estimate of the scaling exponents of all these various contributions is facilitated by the fact that we are interested now in the "local" situation when all the coordinates are of the order of R. Thus, for example, diagram (2) in Fig. 10(a) are redrawn in Fig. 11. The objects in the left grey ellipse in

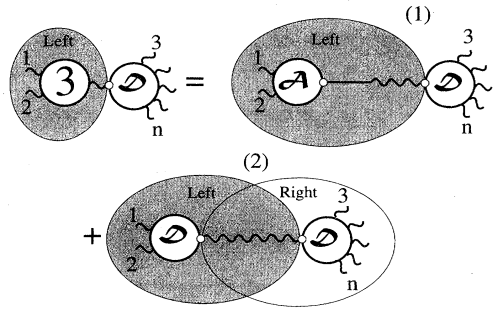

FIG. 11. Diagrammatic representation of the weakly linked contribution for F_n shown as diagram (2) in Fig. 10(a). For the three-point correlator $F_3(\mathbf{r}_0|x_a,x_b,x_c,x_d)$ we used the representation of Fig. 6(c) and placed it here in the dashed ellipse, which is denoted "left." On the right we have an m-point object $\mathscr{D}_m$, which is a generalization for the case $m>3$ of $\mathscr{D}_3$ and appeared in Fig. 1(d).

diagrams (1) and (2) are representations of F_3 shown in Fig. 6(c). The object in the right ellipse of diagram (2) belongs to F_{n-1}. One can see this by taking $n=3$ and looking back to Fig. 6(c). However, in diagram (2) we counted the F_2 bridge twice. The overall scaling exponent is therefore $\zeta_3+\zeta_{n-1}-\zeta_2$. Using Fig. 6(b) it can be also seen that diagram (1) in Fig. 11 has the same scaling exponent. Similarly we can analyze diagram (1) in Fig. 10(a) and argue that its scaling exponent is $\zeta_3+\zeta_{n-1}-\zeta_2$, etc.

Now we need to understand which of these contributions will take the lead if the main scaling $(R/L)^{\zeta_n}$ cancels. To guide our thinking we will assume that the scaling exponents are neither K41 nor β model, but are nonlinear functions of n. Hölder inequalities then require that the increments between ζ_n and ζ_{n-1} will be nonincreasing functions of n, i.e.,

$$\zeta_{n+1}-\zeta_n \leqslant \zeta_n-\zeta_{n-1}. \tag{6.5}$$

With these inequalities one sees that the unlinked contributions that scale with $(R/L)^{\zeta_p+\zeta_q}$ are always smaller than the weakly linked contributions, and that of all the weakly linked contributions the leading one is the one that we singled out in Fig. 10(a), with the scaling exponent $\zeta_3+\zeta_{n-1}-\zeta_2$.

The meaning of this result is that instead of evaluating T_n in the integrals for D_n as $S_n(R)$ we need to evaluate it as $S_{n-1}(R)S_3(R)/S_2(R)$. Correspondingly the evaluation (6.3) changes to

$$D_n(R)=d_n(\zeta_n)\frac{S_n(R)S_3(R)}{RS_2(R)}, \tag{6.6}$$

where $d_n(\zeta_n)$ is a coefficient that depends on the numerical value of the scaling exponent.

VII. ANALYSIS OF THE BALANCE EQUATION AS A NONPERTURBATIVE CONSTRAINT

At this happy moment we can use all the knowledge accumulated so far to go back to the balance equations (2.24) and (2.25) that we rewrite in the form

$$D_n(R)=J_n(R), \tag{7.1}$$

where the forcing term is not displayed because it is negligible, cf. Sec. II C 3. The evaluation of $J_n(R)$ is given by (5.14) and (5.19) in the first and second scenarios, respectively. The evaluation of D_n is either (6.3) or (6.6), depending on whether or not there is cancellation in the leading scaling behavior of D_n. We will show now that each of these evaluations may lead to multiscaling, although linear scaling is not ruled out.

A. Linear scaling: Burgers turbulence and the β model

The evaluation (6.3) is exactly correct only when there is no pressure term and the projection operator is a δ function. This is the situation, for example, in Burgers turbulence [22]. It may or may not be a proper evaluation of D_n also in the case of Navier-Stokes turbulence, as discussed above. We examine now the consequences of this evaluation when substituted in the balance equation with J_n taken from the first scenario. Substituting (6.3) and (5.14) in (7.1) we find

$$\frac{S_{n+1}(R)}{R}\sim\bar{\epsilon}\frac{S_n(R)}{S_2(R)}. \tag{7.2}$$

For $n=2$ we recover the known result that $S_3(R)\sim\bar{\epsilon}R$. Accordingly we can rewrite (7.2) as

$$S_{n+1}(R)S_2(R)\sim S_n(R)S_3(R). \tag{7.3}$$

In terms of the scaling exponents this result reads

$$\zeta_{n+1}+\zeta_2\sim\zeta_n+\zeta_3. \tag{7.4}$$

The only solution of this equation is the linear law $\zeta_n=a+bn$, where a and b are some constants. Knowing that $\zeta_3=1$ and using our scaling law (4.13), which is $\mu=2\zeta_2-\zeta_4$, we find that the only solution is

$$\zeta_n=\frac{n}{3}-\mu\frac{(n-3)}{3}. \tag{7.5}$$

It is interesting to note that this result is identical to the prediction of the β model [20], coefficients and all. This should not surprise us too much. After all, once we have a linear dependence two constraints fix the linear law completely. Note that this law includes as a special case the exponents of Burgers turbulence which are $\zeta_n=1$ for all n [22]. This is obtained from (7.5) when $\mu=1$. Nevertheless the full analysis of the Burgers equation using the techniques developed in this series of papers need special attention due to the importance of the incompressibility constraint in so many of our calculations. The Burgers case deviates so strongly from K41 that the issues of locality and rigidity of the various diagrams needs to be assessed separately [23].

We can also show now that (7.5) implies that the renormalization scale is the outer scale of turbulence L as claimed before. Equation (7.5) was derived by asserting that the Gaussian contribution to J_n is negligible compared to the connected ladder contributions that led to (5.14). The Gaussian contributions are dominated by $\bar{\epsilon}S_{n-2}$ whose scaling exponent is ζ_2. If we used this contribution as the leading one in the balance equation (7.1) we would have obtained the scaling relation $\zeta_{n+1}=\zeta_3+\zeta_{n-2}$ with the obvious boundary

condition $\zeta_0=0$. The solution of this recursion relation is K41 scaling with $\zeta_n=n/3$. If this is to be rejected in favor of (7.5) the Gaussian contributions must be indeed smaller than the ones we kept. The conclusion is that

$$S_2(R)S_{n-2}(R)<S_n(R). \tag{7.6}$$

In turn this inequality implies that

$$\left(\frac{R}{\ell}\right)^{\zeta_{n-2}}<\left(\frac{R}{\ell}\right)^{\zeta_n-\zeta_2}. \tag{7.7}$$

Substituting the scaling exponents from (7.5) we conclude that $(R/\ell)^{\mu}<1$, which can only happen if $R<\ell$ for any R in the inertial interval. This identifies ℓ with L.

B. Multiscaling in the first scenario

Multiscaling in the first scenario can occur only if the leading order evaluation of D_n vanishes identically. Substituting (6.6) and (5.14) in (7.1) we find

$$d_n(\zeta_n)\frac{S_n(R)S_3(R)}{RS_2(R)}=\frac{nJ_2S_n(R)}{2S_2(R)}=\frac{nS_n(R)S_3(R)}{2RS_2(R)}, \tag{7.8}$$

where the last form is obtained from $J_2=S_3/R$. From the point of view of scaling exponents this equation is an identity. The only way to compute the exponents ζ_n now is from the *coefficients* in the balance equation:

$$2d_n(\zeta_n)=n. \tag{7.9}$$

To this aim the rough evaluation of D_n in Sec. VI B is not sufficient; we need to be much more precise in order to compute the ζ_n dependence of d_n.

Clearly, the computation of coefficients is exceedingly hard. Only when we have the exact form for the functional dependence of the many point functions can we hope to compute the coefficient. We did have an exact form for J_n because we understood how to resum its diagrams; consequently we believe that we have computed the coefficient of J_n exactly. D_n is a different matter; at present we do not have an exact functional form for it. Order-by-order considerations are not helpful for this issue, and we still do not know how to exactly resum the diagrammatics for D_n. We will therefore try to guess the ζ_n dependence of the coefficient of D_n. To guide our thinking we recall some results from the theory of passive scalar advection [18,19,24]. In that problem D_n had the form of an eddy-diffusivity operator:

$$D_n^{\text{passive}}(R)=\frac{1}{R^2}\frac{d}{dR}R^2h(R)\frac{d}{dR}S_n(R), \tag{7.10}$$

where $h(R)$ is the eddy diffusivity, which scales with R as a power law R^{ζ_h}. Can we use this to guess a form for $D_n(R)$ in the present case? On the face of it the answer is no. Our evaluation (6.3) indicated that if we have a differential operator it operates on S_{n+1} rather than on S_n. On the other hand, once we assume that the leading order evaluation cancels in D_n, the next order is again in terms of S_n as in the case of passive scalar. In fact, it is not difficult to see (Appendix) that the topology of the weakly linked diagrams for D_n is identical (after the cancellation of the leading order) to the topology of the leading contributions for D_n in the case of the passive scalar. We thus guess that for the aim of evaluation of the coefficient we can write $D_n(R)$ with an eddy viscosity similar to (7.10) in which $h(R)$ is found by comparing (7.10) and (6.6):

$$D_n(R)=b\frac{1}{R^2}\frac{d}{dR}R^2\frac{S_3(R)R}{S_2(R)}\frac{d}{dR}S_n(R), \tag{7.11}$$

with b being now an n-independent coefficient. The physical meaning of this guess is that the R-dependent eddy viscosity $h(R)$ here takes the form

$$h(R)=b\frac{RS_3(R)}{S_2(R)}. \tag{7.12}$$

Note that the eddy diffusivity that is introduced here scales as $R^{2-\zeta_2}=R^{\Delta}$.

Using (7.11) we compute

$$d_n(\zeta_n)=b\zeta_n(3+\zeta_n-\zeta_2), \tag{7.13}$$

where we used the fact that $\zeta_3=1$. Together with (7.9) we find a quadratic equation for ζ_n:

$$2b\zeta_n(3+\zeta_n-\zeta_2)=n. \tag{7.14}$$

We remind the reader that this equation is valid for $n>2$ since there is no cancellation of the leading scaling order in D_2. Using again the fact that $\zeta_3=1$ we find the constraint

$$2b(4-\zeta_2)=3. \tag{7.15}$$

This leaves us in (7.14) with only one unknown number, which we take as ζ_2. Solving for ζ_n we find

$$\zeta_n=\frac{3-\zeta_2}{2}\left[-1+\sqrt{1+\frac{4n(4-\zeta_2)}{3(3-\zeta_2)^2}}\right]. \tag{7.16}$$

Comparing this result with experimental data, one can see that it gives an acceptable description of ζ_n for $n<10$. We do not claim, however, that this result is exact or even qualitatively correct. Our main aim had been to understand how multiscaling may appear and how the outer scale shows up as the renormalization scale. This aim is achieved in this scenario and in the second scenario as well. These scenarios differ in the asymptotic predictions for ζ_n for large n. In the present case for large n ζ_n goes like $\sqrt{n}$. The second scenario predicts asymptotic linear dependence on n (but with nonlinear dependence for small n).

C. Multiscaling in the second scenario

Multiscaling occurs in the second scenario if D_n is correctly evaluated by Eq. (6.6). Using this and (5.19) we find

$$\frac{b_n\zeta_{n+1}S_{n+1}}{R}=\frac{J_2nS_{n+1}}{2S_3}. \tag{7.17}$$

For $n=2$ the evaluation (6.6) is exact with $b_2=1$. This means that $J_2=S_3/R$. Using this we get finally

$$2b_n\zeta_{n+1}=n. \tag{7.18}$$

Armed with our understanding that b_n is likely to become n independent for large n we see that in this scenario ζ_n becomes asymptotically linear in n.

Analyzing the integrals (2.36) and (2.37) taking into account the known asymptotic behavior of the T tensors one can propose a plausible n interpolation formula for b_n. This will lead to a model for ζ_n. However, our main aim in this paper has been the elucidation of the mechanism for multiscaling rather than the numerical values of ζ_n. We prefer to postpone this issue to a moment in which a better understanding of the viscous cutoffs will be achieved.

VIII. CONCLUDING REMARKS FOR PAPERS I–III AND THE ROAD AHEAD

We believe that the theory that was presented in papers I–III contains elements that are likely to remain cornerstones in the theory of the fine structure of hydrodynamic turbulence. Since the approach is highly technical, we attempt in these concluding remarks to summarize first what are the essential elements of the analysis from the point of view both of technique and of physics.

Our conceptual approach to the analytic theory of fully developed turbulence rests on three main steps, which are roughly associated with papers I, II, and III. The first step is the proof of locality of eddy interactions, which furnishes a precise meaning to the Richardson-Kolmogorov cascade picture. The second step consists of the derivation of anomalous scaling of fields involving second and higher spatial derivatives. We exposed the explicit appearance of anomalous exponents with the ultraviolet cutoff length as the renormalization scale. It is intuitively clear that gradient fields cannot be insensitive to η since by definition a gradient measures differences on scales smaller than η, and this length may appear when one attempts to calculate the correlation functions of gradient fields. Indeed, an important step in our theory is the explicit identification of the ultraviolet divergences, which appear in the diagrammatic theory of correlations of gradient fields, and the computation of the largest anomalous exponent associated with such divergences. The third step addressed (in the present paper) the origin of anomalous scaling of the structure functions with the outer scale acting as the renormalization scale. The outer scale appears in the "boundary conditions" in the space of scales on the fully resummed series. It is not completely evident that our route is either economical or unique. This route reflects the nature of our understanding and the path followed by us, and it is possible that there is a shorter path to the same results. Only future research will tell us about that.

Let us summarize the technical aspects of our analysis. The foundation of the theory is the Navier-Stokes equations. Starting from these equations we use a combination of renormalized (but order by order) analysis of diagrammatic perturbation series with some exact, nonperturbative considerations. We found that only the latter allowed us to derive multiscaling. Order-by-order analysis could not take us out of the traditional K41 scaling laws.

The scale invariant formulation of diagrammatic perturbation theory for fluid mechanics to all orders becomes technically tractable due to the Belinicher-L'vov transformation of the Eulerian velocity field. Without it, all known approaches are either plagued by infrared divergences or are limited to low order perturbation terms. In paper I we developed a Wyld-type diagrammatic technique for BL velocity differences in $\mathbf{r},t$ representation. This presentation allows one to consider a pth order diagram for the structure function $S_n(R)$ as a set of "elementary" interactions involving p intermediate points with integration over their space-time coordinates. One important discovery of paper I is the *property of locality*, which means that the major contribution to these integrals originates from a *ball of locality*, which is a sphere of radius of the order of R. In physical language locality is equivalent to the cascade picture of Richardson. Indeed, locality means that the eddies of scale R interact mostly with motions of comparable scales, while the direct effect of motions on the scales L or η are negligible when these are much larger (or respectively smaller) than R. A direct consequence of locality is that perturbative techniques cannot uncover deviations from normal K41 scaling of $S_n(R)$. Anomalous scaling must result, if it exists, from nonperturbative effects.

The main result of paper II is the nonperturbative demonstration of the existence and origin of anomalous exponents stemming from the ultraviolet scales [13,14]. As in the theory of second order phase transitions there is a logarithmic divergence in the uv regime of ladder diagrams for correlation functions of velocity *gradients*. Anomalous behavior appears as a nonperturbative solution of some formally exact diagrammatic equation, which one obtains after resumming the ladder diagrams. Physically, anomalous behavior of correlation functions with two (or more) very different separation distances $r \ll R$ is the result of a summation over a large number $\mathcal{N}=(R/r)^{\Delta}$ of equally important channels of interaction of turbulent motions having scales between r and R. The main achievement of paper II is the computation of the anomalous scaling exponent Δ and it was found that Δ exactly equals its critical value $\Delta_{\rm cr}=2-\zeta_2$. This fact is of crucial importance for the nature of anomalous scaling of the structure functions in hydrodynamic turbulence. In the hypothetical case $\Delta<\Delta_{\rm cr}$ one expects K41 scaling of the structure functions in the limit $\mathrm{Re}\to\infty$. There can be only subcritical corrections to this, and such corrections have the *viscous scale* η as the renormalization scale. In reality $\Delta=\Delta_{\rm cr}$ and this opens up the possibility for the destruction of K41 for all values of Re.

The analysis of the possible mechanisms for anomalous (non-K41) scaling of the structure function is the main topic of paper III. The main theoretical question was how the outer scale L appears in the theory. The answer that we offered above is that this scale appears when one resums the series for the structure functions. Although each term converges when $L\to\infty$, the sum diverges. Accordingly, one needs a nonperturbative constraint on the whole series in order to proceed. Our analysis is based on the exact and nonperturbative *balance equations* $D_n(R)=J_n(R)$, which follow from the equation of motion for the structure functions $S_n(R)$. These equations are a direct consequence of the Navier-Stokes equations in the statistical stationary state in which $\partial S_n(R,t)/\partial t=0$. We presented two evaluations of the viscous term $J_n(R)$, depending on the nature of the viscous cutoffs. In the first scenario there exists only one viscous scale, as in the K41 theory. The second scenario allows a more realistic multiplicity of viscous scales depending on

which quantity is analyzed. In both scenarios multiscaling can be realized. They differ in the asymptotic dependence of ζ_n on n (such as $\sqrt{n}$ or linear in n, respectively), but the basic mechanism for the appearance of the outer scale is the same.

One particularly pressing subject for future research is the asymptotic behavior of n order correlation functions. We found in the present paper that when two of the coordinates of $F_n(\mathbf{r}_1,\mathbf{r}_2,\ldots,\mathbf{r}_n)$ (say $\mathbf{r}_1$ and $\mathbf{r}_2$) coalesce, the correlation function is proportional to $S_2(r_1)$. This is just one example of the asymptotic properties that are summarized under the term "fusion rules." We need to understand the deep structure of the theory that is responsible for this fusion rule, but that will also allow us to predict what happens, say, when three or more points coalesce. We guess that the n-point correlation function in that case will be proportional to F_3, etc. Formally we need to discuss the operator algebra that will automatically furnish all the needed fusion rules, and will be also compatible with multiscaling. We plan to propose elements of such a theory in a forthcoming publication [17]. Of course, as far as the actual computation of scaling exponents is concerned, the most important missing element is a knowledge of the viscous scale of such quantities. In other words, when p out of say n points coalesce together, and the $n-p$ points remain R away from each other, when does the behavior of the function $S_p(r)$ cross over to dissipative scaling. That viscous scale may have an R dependence, and we need to know that R dependence to achieve a first principle calculation of the scaling exponents. Finally, we comment on the relation and differences between scaling in turbulence and scaling in better understood subjects like critical phenomena. Because of the superficial similarities (many body problems with strong interaction and scale invariance) there were many attempts to apply formal schemes in the wake of critical phenomena to understand turbulence: renormalization groups, ϵ expansion, $1/d$ expansion, $1/N$ expansions, and what not. If the approach taken in this series of papers turns out to be correct, this will mean that the theory of turbulence is significantly different from critical phenomena. Some elements reappear: sums of ladder diagrams contribute anomalous exponents, fusion rules are needed, and the possibility of operator algebra is there.

However there are at least two major differences: there exists flux equilibrium instead of thermodynamic equilibrium, and the interaction in the theory of turbulence is highly nonlocal because of the effects of pressure. In contrast, in critical phenomena it is sufficient to have local interactions that build up to global criticality because of the cancellation of energetic and entropic contributions to the free energy. In turbulence, notwithstanding the nonlocality of the interaction, it turns out that the diagrammatic theory in BL variables is finite order by order. In contrast, the perturbative analysis of critical phenomena leads to divergences that result (after renormalization) in anomalous scaling. Thus the mechanism for anomalous scaling in turbulence must be different.

Due to the flux equilibrium there is a global connection between the largest and smallest scales in the problem. A deep consequence of the flux equilibrium is the two-point fusion rule that was discussed above as one of the cornerstones for multiscaling. In addition, flux equilibrium and the need to satisfy boundary conditions at the two ends of the energy cascade introduce the possibility of having the outer scale as the renormalization length *without* infrared divergences in order-by-order expansions for the structure functions.

As a result of all these differences we do not have the fixed point structure with a small number of unstable directions that is so typical of critical phenomena. In some sense, the independence of the perturbative terms from a typical scale means that we have an infinite number of *marginal* operators. The resummation of the perturbative theory results in a possibility of dressing these marginal operators, and there can be infinitely many independent exponents. Whether such a concept can be turned into a computational scheme is a question for the future.

ACKNOWLEDGMENTS

We thank Mark Nelkin and Bob Kraichnan for useful remarks concerning the viscous cutoffs and universality. This work has been supported in part by the U.S.–Israel Binational Science Foundation, the German-Israeli Foundation, and the Naftali and Anna Backenroth-Bronicki Fund for Research in Chaos and Complexity.

APPENDIX: WEAKLY LINKED CONTRIBUTIONS TO THE INTERACTION TERM

In this appendix we discuss the weakly linked contributions to the interaction term D_n. In Eqs. (2.36) and (2.37) the integrals depend on the $(n+1)$-order correlation function $T_{n+1}(\mathbf{r},\mathbf{r},\mathbf{R})$ in which the two first coordinates $\mathbf{r}$ are special (they are either $\mathbf{r}_1$ or $\mathbf{R}+\mathbf{r}_1$ and there is a derivative with respect to $\mathbf{r}_1$). In its turn every weakly linked contribution to $F_{n+1}(\mathbf{r}_1,\mathbf{r}_2,\ldots,\mathbf{r}_{n+1})$ [or to $T_{n+1}(\mathbf{r},\mathbf{r},\mathbf{R})=F_{n+1}(\mathbf{r},\mathbf{r},\mathbf{R},\mathbf{R},\ldots,\mathbf{R})$] has two weakly linked legs [denoted in Fig. 10(a) as x_a,x_b], connected to the body of the diagram via a one-propagator bridge. There are $C_{n+1}^2=n(n+1)/2$ weakly linked contributions to F_{n+1} in which the role of weakly linked legs is played by each pair taken from the $n+1$ total number of legs. The C_{n+1}^2 contributions to D_n can be subdivided into three groups. The first group consists of just one term in which two special coordinates in T_{n+1} are exactly the coordinates of the two weakly linked legs ($\mathbf{r}=\mathbf{r}_a=\mathbf{r}_b$). The second group of terms in D_n has $2(n-1)$ terms in which just one of the special coordinates in T_{n+1} (but only one of the two) is associated with a weakly linked leg. The second special coordinate is free to be associated with any of the $(n-1)$ legs of the body of the weakly linked diagram for F_{n+1}. This body is an n-point object [see Fig. 10(a)] in which one leg is used to create the bridge. The last (third) group of terms in D_n has $C_{n-1}^2=(n-1)(n-2)/2$ terms in which two special T coordinates may be chosen from the coordinates of any $(n-1)$ free legs in the body of the weakly linked diagram for F_{n+1}.

The first two groups of terms correspond exactly to the topology of the diagrammatic representation of the interaction term D_n in the problem of turbulent advection of a passive scalar field $T(\mathbf{r},t)$; cf. Sec. V B in [24] and Sec. II B 2 in [19]. Consider Fig. 10 of [24]. The dashed lines in this figure represent two-point velocity correlators, and these are

replaced in our case by wavy correlator lines. The wavy lines in the passive scalar case represent two point scalar correlators, and they remain as wavy lines in the present case. The fragment of the diagram in this figure that is placed to the right of the legs denoted by q_2, q_3, q_4 and to the right of the vertex between k and q_1 must be interpreted now as a contribution to the strongly linked four-point velocity correlator. The last serves a a four-point body of a weakly linked contribution to a five-point velocity correlator F_5. We thus conclude that the topology of the diagrams for D_n in the case of turbulent passive advection and the first two groups of weakly linked diagrams for D_n in the case of Navier-Stokes turbulence is the same.

It appears that the third group of C_{n-1}^2 terms that we described above forms a major difference between the problems of turbulent advection and Navier-Stokes turbulence. In fact this group does not contribute. In the case of passive scalar this group is absent because of the zero value of the $\langle Tv \rangle$ correlator. It is remarkable that in the present case of Navier-Stokes turbulence this group cancels under the same condition of cancellation of the leading (strongly linked) contributions to D_n. These terms may be considered (after severing the bridge to the weakly linked fragment) as strongly linked contributions to D_{n-1}. They must cancel if the scenario leading to multiscaling is assumed.

The conclusion of this appendix is far from being trivial, and in some sense is very surprising. It says that although the passive advection problem is linear and local, whereas Navier-Stokes in nonlinear and nonlocal (pressure), it appears that if multiscaling is expected, the topology of the diagrams for D_n is very similar in the two cases. If this is correct, it must be related to some deep symmetry. If so, the eddy viscosity approximation used in Sec. VII may contain some essential aspects of the truth.

[1] V. S. L'vov and I. Procaccia, in Lecture Notes of the Les Houches 1994 Summer School, 1995, edited by F. David and P. Ginsparg (North-Holland, Amsterdam, 1995).
[2] V. S. L'vov and I. Procaccia, Phys. Rev. E **52**, 3840 (1995).
[3] V. S. L'vov and I. Procaccia, Phys. Rev. E **52**, 3858 (1995).
[4] A. N. Kolmogorov, Dokl. Akad. Nauk SSSR **30**, 229 (1941).
[5] A. S. Monin and A. M. Yaglom, *Statistical Fluid Mechanics* (MIT Press, Cambridge, 1975), Vol. 2.
[6] M. Nelkin, Adv. Phys. **43**, 143 (1994).
[7] Uriel Frisch, *Turbulence: The Legacy of A.N. Kolmogorov* (Cambridge University Press, Cambridge, 1995).
[8] K. R. Sreenivasan and P. Kailasnath, Phys. Fluids A **5**, 512 (1993).
[9] H. W. Wyld, Ann. Phys. **14**, 143 (1961).
[10] P. C. Martin, E. D. Siggia, and H. A. Rose, Phys. Rev. A **8**, 423 (1973).
[11] C. De Dominicis and L. Peliti, Phys. Rev. B **18**, 353 (1978).
[12] V. I. Belinicher and V. S. L'vov, Zh. Éksp. Teor. Fiz. **93**, 1269 (1987) [Sov. Phys. JETP **66**, 303 (1987)].
[13] V. S. L'vov and V. V. Lebedev, Europhys. Lett. **29**, 681 (1995).
[14] V. V. Lebedev and V. S. L'vov, Pis'ma Zh. Éksp. Teor. Fiz. **59**, 546 (1994) [JETP Lett. **59**, 577 (1994)].
[15] V. S. L'vov and I. Procaccia, Phys. Rev. Lett. **74**, 2690 (1995).
[16] G. L. Eyink, Phys. Lett. A **172**, 355 (1993).
[17] V. S. L'vov and I. Procaccia (unpublished).
[18] R. H. Kraichnan, Phys. Rev. Lett. **72**, 1016 (1994).
[19] A. L. Fairhall, O. Gat, V. S. L'vov, and I. Procaccia, Phys. Rev. E **53**, 3518 (1996).
[20] Uriel Frisch, Pierre-Louis Sulem, and Mark Nelkin, J. Fluid Mech. **87**, 719 (1978).
[21] A. N. Kolmogorov, J. Fluid Mech. **13**, 82 (1962).
[22] T. Gotoh, Phys. Fluids **6**, 3985 (1994).
[23] A. N. Polyakov, Phys. Rev. E **52**, 6183 (1995).
[24] V. S. L'vov, I. Procaccia, and A. Fairhall, Phys. Rev. E **50**, 4684 (1994).
[25] R. Benzi, S. Ciliberto, C. Baudet, and G. Ruiz Chavarria, Physica D **80**, 385 (1995).
[26] G. Stolovitzky, K. R. Sreenivasan, and A. Juneja, Phys. Rev. E **48**, R3217 (1994).
[27] J. Herweijer and W. van de Water, Phys. Rev. Lett. **74**, 4651 (1995).

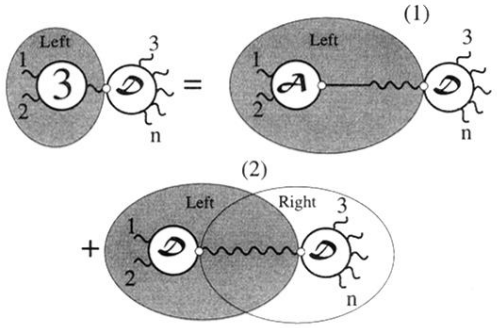

FIG. 11. Diagrammatic representation of the weakly linked contribution for F_n shown as diagram (2) in Fig. 10(a). For the three-point correlator $F_3(\mathbf{r}_0|x_a,x_b,x_c,x_d)$ we used the representation of Fig. 6(c) and placed it here in the dashed ellipse, which is denoted "left." On the right we have an m-point object $\mathscr{D}_m$, which is a generalization for the case $m>3$ of $\mathscr{D}_3$ and appeared in Fig. 1(d).